Nanoscale Advances

ROYAL SOCIETY OF CHEMISTRY

REVIEW

View Article Online
View Journal | View Issue

Cite this: *Nanoscale Adv.*, 2023, **5**, 3177

Accounts of applied molecular rotors and rotary motors: recent advances

Anup Singhania, [ab] Sudeshna Kalita, [ab] Prerna Chettri [ab] and Subrata Ghosh *[ab]

Molecular machines are nanoscale devices capable of performing mechanical works at molecular level. These systems could be a single molecule or a collection of component molecules that interrelate with one another to produce nanomechanical movements and resulting performances. The design of the components of molecular machine with bioinspired traits results in various nanomechanical motions. Some known molecular machines are rotors, motors, nanocars, gears, elevators, and so on based on their nanomechanical motion. The conversion of these individual nanomechanical motions to collective motions *via* integration into suitable platforms yields impressive macroscopic output at varied sizes. Instead of limited experimental acquaintances, the researchers demonstrated several applications of molecular machines in chemical transformation, energy conversion, gas/liquid separation, biomedical use, and soft material fabrication. As a result, the development of new molecular machines and their applications has accelerated over the previous two decades. This review highlights the design principles and application scopes of several rotors and rotary motor systems because these machines are used in real applications. This review also offers a systematic and thorough overview of current advancements in rotary motors, providing in-depth knowledge and predicting future problems and goals in this area.

Received 4th January 2023
Accepted 17th May 2023

DOI: 10.1039/d3na00010a

rsc.li/nanoscale-advances

1. Introduction

1.1. Translation of chemical structure to molecular machine

Chemical structures often account for the execution of chemical reactions associated with the chemical state change of the molecules; nature's kitchen uses chemical reactions and biosynthesis processes to produce an innumerable number of molecules. Besides these, nature has specific ways of organizing biological processes with various regulatory tools.[1–3] One such tool is biomolecular machines that execute jobs by changing their conformational states and using their programmed mechanical dynamics. Though there is hardly any difference in the chemical structures of machines and non-machines, these molecular machines show real-time operations to execute many routine biological jobs. The most miniature proton-driven biomolecular motor is F_1-ATPase, a γ-subunit of ATP synthetase enzyme that works as a central

[a]*Natural Product Chemistry Group, Chemical Sciences & Technology Division, CSIR-North East Institute of Science & Technology, Jorhat, 785006, Assam, India. E-mail: ocsgin@gmail.com*

[b]*Academy of Scientific and Innovative Research (AcSIR), Ghaziabad, 201002, India*

Anup Singhania is a Research Scholar pursuing his PhD under AcSIR at CSIR-North East Institute of Science and Technology, Jorhat, India. He has completed his graduation (BSc) from Dibrugarh University and received his MSc degree in Chemistry from North–Eastern Hill University, Shillong, India. His research focuses on developing new molecular motors for applications in energy harvesting, resonance drug development, and other relevant areas.

Sudeshna Kalita is pursuing her PhD under AcSIR, Ghaziabad, at CSIR-North East Institute of Science and Technology, Jorhat, India. She completed her undergraduate (BSc) degree in 2016 with honors in Chemistry and obtained her postgraduate (MSc) degree from Dibrugarh University, India, in 2018. Her research focuses on the design and synthesis of molecular motor-based soft actuators and smart materials.

rotor. It processes unrestricted angular rotatory motion of the subunit surrounding a $\alpha_3\beta_3$stator and reverses ATP synthesis and hydrolysis.[4] Thereby, the knowledge of molecular machines came, and it categorically refers to groups of chemical structures with remarkable potential to produce mechanical forces and accomplish measurable physical works. Molecular machines[5,6] are generally subclassed into rotors, motors,[7] rotaxanes, catenanes,[8,9] and some typical switches.[10] Synthetic chemists started mimicking the biological molecular machines and using biomimetic nanomechanical mechanisms to build artificial molecular machines. They focused on the control of the directional movement processes of the molecule. Investigations have shown the different modes of operation and control of molecular machines in different environments.[11–13]

The advancement was significantly accelerated when scientists learned to synthesize mechanically interlocked molecules.[14] The concept of nanotechnology by Richard Feynman was well-established by Jean-Pierre Sauvage, Sir Fraser Stoddart, and B. L. Feringa through their contribution to molecular machines.[15–18] We found several biomachines in nature, but deciphering their exact mechanisms is complex. However, researchers have successfully decoded the mode of action of natural motor proteins in the last few decades. Depending on the unique properties of biomachines, the molecular systems were classified[6,8,19] earlier based on the types of work they served. For example, a switch-based molecule has reversible movements, and the relative positions of different molecular parts influence the state of the switch. The molecule can undo the switch effect when the molecular counterparts return to the initial position. A molecular motor impacts systems by operating their components or a substrate over the trajectory. Motor function is repetitive and progressive in a system.[6,19]

However, the switches can be a motor in a particular condition if the "forward" transition between two states takes a different route than the "backward" transition.[8] In this context, Feringa's unidirectional overcrowded alkene motor is an example.

1.2. Molecule motors and their motion

After the discovery of Brownian motion in 1827 by the famous botanist Robert Brown, Einstein and Perrin proved that the bombardment by the particles available for collision with the molecule instigated Brownian motion.[20–23] With the growing interest in building molecular machines, scientists have made numerous efforts to understand artificial molecular machines and their modes of action by synthesis and characterization. Brownian motor-type machinery is found in nature in the curved movement of eggs in the fallopian tube.[24–26] The egg progression occurs by systematically regulating the outer and inner dynein arms in the fallopian tube. Three biomolecular motor classes in eukaryotic cells generate power *via* their stochastic linear movements: actin-based myosin band motor proteins, tubulin-based dyneins, and kinesin motor proteins. These proteins bind to the specific nucleotide, leading to a change in the conformation due to ATP hydrolysis.[27–30] Actin-based protein myosin hydrolyzes ATP; it generates force through the power stroke (PS) mechanism in skeletal muscle that walks toward the positive end of an actin filament and causes muscle contraction.[31,32] Similarly, other motor proteins play a vital role in cellular functions: transporting intracellular cargo to the specific site, synthesizing proteins, replicating DNAs, and decoding the DNA strands.[33–36]

Motor proteins have been extensively used in nanofabrication and as building blocks for generating hybrid systems by engineering synthetic molecules.[37–39] These

Prerna Chettri is a PhD research scholar under AcSIR, Ghaziabad, at CSIR-North East Institute of Science and Technology, Jorhat, Assam, India. She completed her BSc and MSc in Zoology from the University of North Bengal, West Bengal, India, in 2016 and 2018, respectively. Her research focus includes nanorobotic drug development for cancer and infectious diseases and bioimaging molecules.

Subrata Ghosh is Principal Scientist at CSIR-North East Institute of Science & Technology Assam, India and Associate Professor of Chemistry at the Academy of Scientific & Innovative Research (AcSIR), Ghaziabad, India. He completed his PhD in 2010 from the Indian Association for the Cultivation of Science (IACS), Kolkata and his degree was awarded by Jadavpur University, Kolkata. He has done postdoctoral research with Dr Anirban Bandyopadhyay at National Institute for Materials Science (NIMS), Tsukuba, Japan and Professor Rudolph E. Tanzi at Massachusetts General Hospital (MGH) & Harvard Medical School (HMS), Boston, USA. His research interest includes double-ratchet motors, molecular switches & computing, smart materials, nanorobotic drug discovery, and neurophysiology & neurodegenerative disorders.

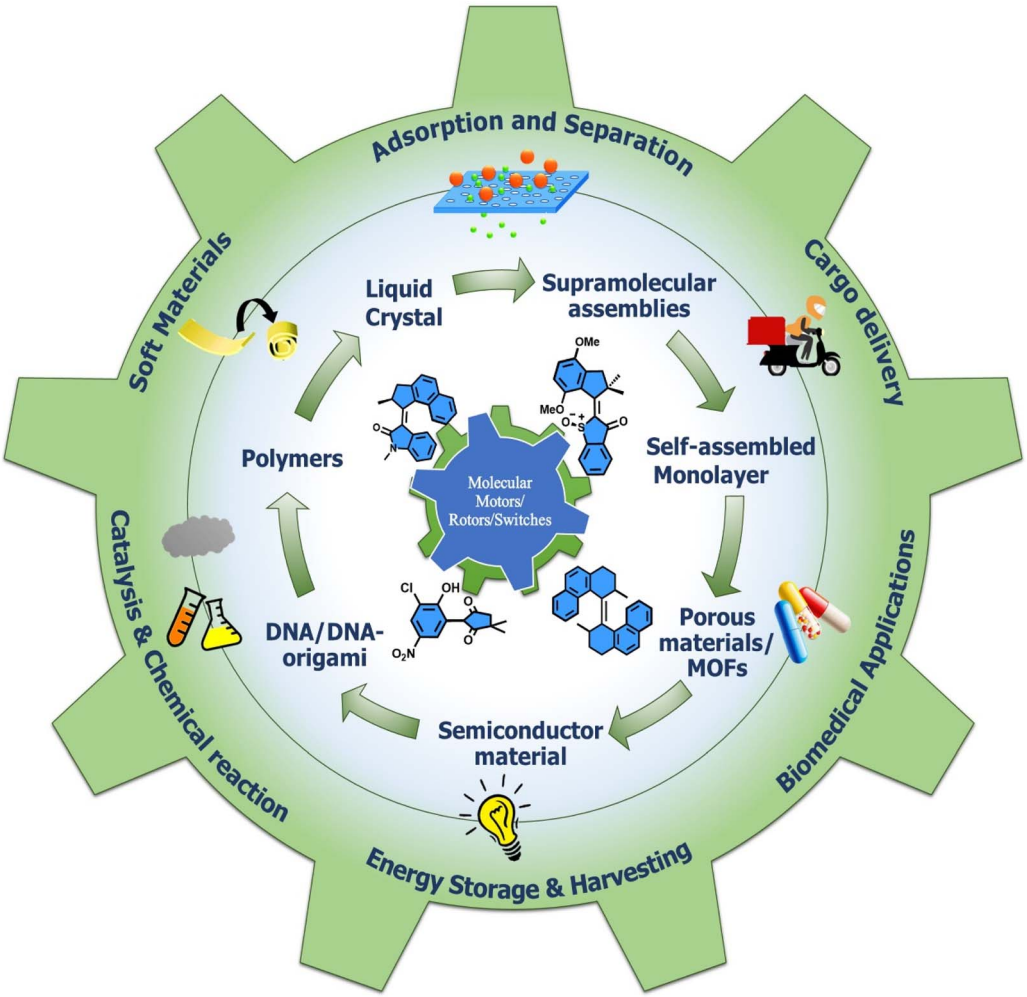

Chart 1 An initial image of molecular rotors/motors and their respective applications.

biomolecular machines comprise amino acid chains that undergo self-assembly or folding utilizing ATP as fuel. DNA scaffolds are used as a tool to arrange/self-assemble the molecular motors, where DNA serves as fuel.[40] Notably, different molecular motors/rotors are linked with DNA origami, where DNA is used to template or drive the assembly of molecular motors. Thus, taking advantage of the complementary base–pair interaction in oligonucleotides and the self-assembly process, DNA-based machines have been developed.

This review focuses on information about the molecular motors' physical and chemical characteristics. We emphasize the development of various rotary motor systems with mechanical properties and their microscopic and macroscopic works (Chart 1). We discuss how the molecular engineering of these motors can allow the building of new hybrid nanodevices that deliver relevant outcomes. Moreover, the collective macroscopic works are highlighted upon integrating with different surfaces or interfaces (such as polymers and 3D porous materials). We kept our discussion centered on rotary motor systems because we found they have the most practical applications. Therefore, some current reviews[6,8,41–43] by eminent contributors have been discussed in depth for the readers' interest.

1.3. Brownian ratchet and power stroke motions

The first and second laws of thermodynamics gave us the knowledge of energy transportation that determines the direction of motion of a body; these laws are valid for macroscopic systems. However, many microscopic biomolecular motors govern the net directional motion in a biological system; thus, it is doubtful whether these two laws are relevant in the molecular domain. A motor protein uses the thermal energy, kT, to produce the directed motion, which conflicts with the second law of thermodynamics. Here, a ratchet mechanism is introduced to describe the phenomenon that governs biomolecular motors' function, generally mentioned as Brownian ratchet (BR) and power stroke (PS) rotors.[44] This mechanism results in a net directional motion when the system is in symmetric potential with directionless applied force. Therefore, the question is how far these macroscopic laws govern the nanomachines in a nonequilibrium environment. The experimental and theoretical investigations strengthen the field of Brownian rotor that

gives an insight into the mechanism.[45] Several other published reviews[6,8,19,46] on molecular machines have vividly consolidated the discussion on these motors' design and working mechanisms. Therefore, we would like to give brief details about some selected interpretations of the same and extend further toward their working principle, potential applications, and future outlook.

A BR is a conceptual machine where an axel connected to a ratchet wheel allows the wheel system to rotate 360° around the axis in the forward direction with a reverse rotation restriction. Such ratchets get power by absorbing random thermal energy from the available sources. However, we may come to specific points where such motion appears highly unrealistic, although the working mechanism is the same. In nature, the BR mechanism assists many intracellular parasites in moving forward in their host system. The motion of a motile bacteria that move forward in the suspension fluid occurs at a low Reynolds number. The working principle of the F_0F_1 rotary motor of ATP synthase was explained with a model that shows how two BR states of the F_1 motor utilize the elastic energy to induce the production of ATP, competing with the F_0 motor to perform complex tasks.[47] The F_1 motor works as a PS using ATP as its fuel. In contrast, the F_0 motor hydrolyzes the ATP and uses the chemical energy against the concentration gradient to rectify the F_1 rotational motion. Efforts have been made to build artificial molecular motors by mimicking these ratchet mechanisms; however, the complexity and design of the biological rotors are stochastic and event-based. Hence, theoretical investigations are helpful and offer insight into the fundamental principles of making the molecules motorized. In another study, Astumian described a unidirectional Brownian motor motion of a large ring that became operational in adiabatic conditions at near equilibrium at every instant,[48] resulting in about efficiency 100%. Eventually, two basic parameters are required for the molecule to become a Brownian rotor: one is self-propelled motion at a low Reynold number, and the other is that the motor should utilize Brownian motion rather than fighting against it because the temperature is not an adequate parameter as the velocity of the system is proportional to the square root of the temperature.[49] Thus, an applied torque is needed for the rotary motor to perform a rotational motion and to repeat mechanical performance. These features must be fitted in a system to design a motor or rotor. Thus, a molecular motor will perform the net-directed motion in potential asymmetric barriers by combining the effect of structural asymmetry and diffusion motion by manipulating the energy barrier at nonequilibrium.[50–52]

The role of kinetic parameters is demonstrated by a comparative study between macroscopic and microscopic tasks, where an example of the movement of the brick from the lower staircase to the upper staircase is performed in two mechanistic ways.[53] Moving the brick from white to black must work against friction that causes energy dissipation irreversibly, whereas lifting the brick into the next staircase is done reversibly (Fig. 1a–c). The modulation of surface friction manipulates this energy dissipation, and this process can be correlated with the modulation of microscopic work exploiting thermal noise and diffusion. The microscopic brick moves forward due to diffusion; moreover, the thermal activation causes the brick to move into the next staircase, whereas chemical energy is utilized to block the backward movement. However, the initial state of the brick is thermodynamically favorable compared to the kinetically stable final state, ascribed to the modulation of the energy barrier, known as the information ratchet. This information ratchet of the Brownian motor is explained by the catalytically driven state of the motor undergoing thermal activation, and diffusion is depicted.

The complex performance of a molecular machine needs to have multiple functional components collectively work in coherence. Different parts of the machine may work in a parallel or stepwise manner. For example, when the ratchet mechanism has different characteristics, *i.e.*, PS and BR, depending on their periodicity and energy inputs, multiple ratchets can possibly combine in a single system to build a motor that works to produce complex tasks (Fig. 1d).[54,55] Biological motor proteins, *e.g.*, Kinesin-1, Myosin-V, and F_1-ATPase, employ these PS and BR mechanisms to a different extent to perform individual biological functions. Thus, combining these two mechanisms makes it possible to deduce a complex motion in a synthetic motor. Generally, we discuss PS and BR mechanisms as two separate ratchet behaviors of a motor protein. However, a clear consensus on their exact nature of work is yet to be known.

1.4. Rationale of double ratchet rotor/motor technology

We define a PS as a significant downhill free energy gradient generated over a distance more significant than the step size.[56] A protein with this sufficiently large gradient may show a strong bias to move against the load.[57] Therefore, the forward transition of a PS is nearly an irreversible process. It is similar to a relaxation of stored elastic potential energy from a strained state along with a nanometer-scale conformation change. Moreover, a BR mechanism follows a thermal gradient for forwarding movement. It stabilizes the position in a stepwise manner *via* the corresponding conformational changes utilizing the fuel processing events.[54,55] However, a small backstroke or limited reversibility produces a stepper motion. An artificial molecular motor is thus created by combining PS and BR functional units in a single system, resulting in a double ratchet rotor (Fig. 1e).[58] These two modules are connected so that BR independently diffuses to a stepper movement within a long temperature range. Such a BR motion can harvest natural energy from thermal fluctuation and engenders a favorable situation to store the energy. For this reason, the adjoint PS module can use the energy as elastic energy to favor the PS to move. Thus, the overall system behaves like a motor running under a long-range free energy gradient. In this current rotor, BR and PS modules are divided into two separate aromatic planes connected through a carbon–carbon triple bond in the current system. The naphthalene plane acts as a string in the PS

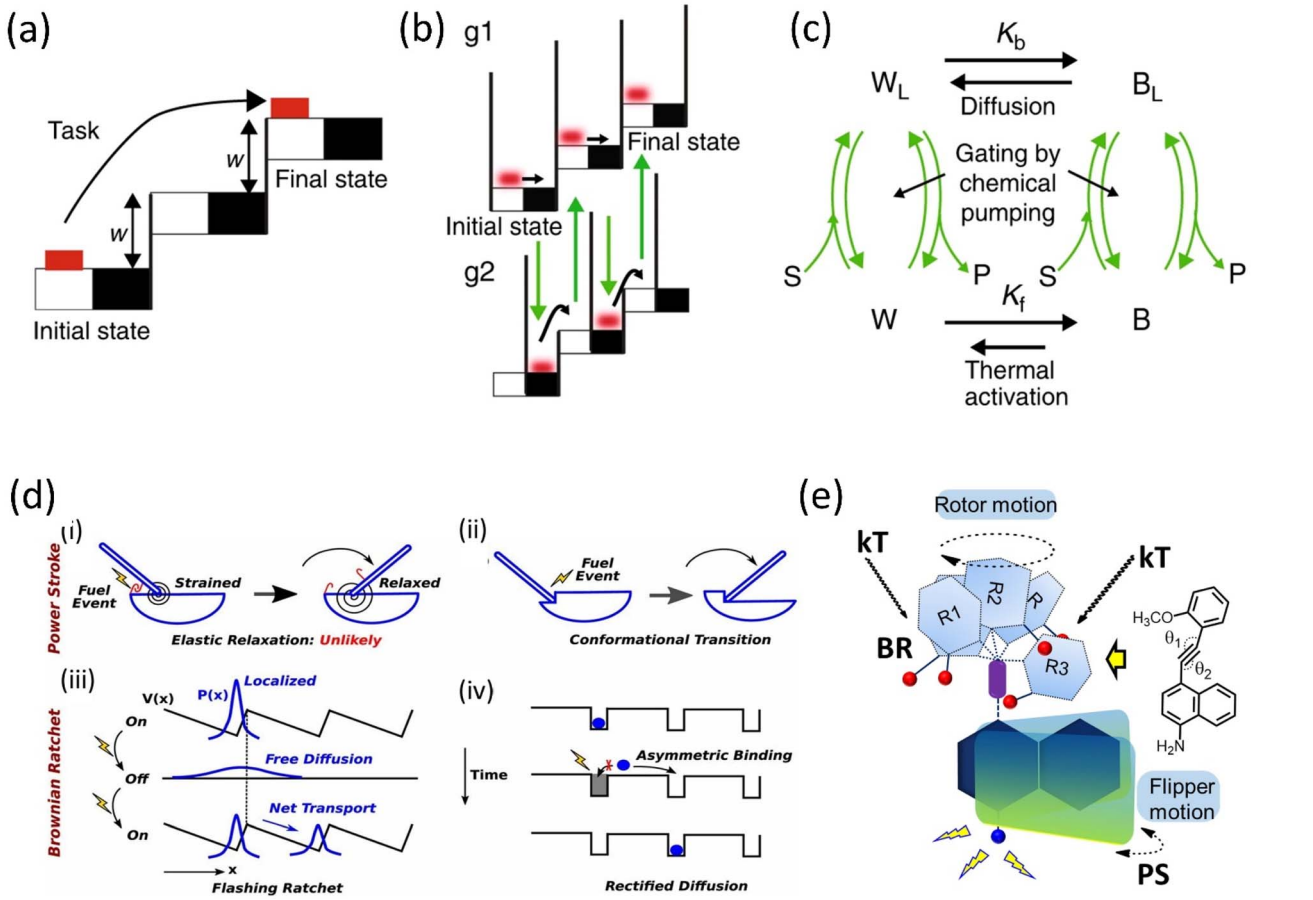

Fig. 1 Graphical representation of (a) a macroscopic task with an example of the movement of a brick and (b) a microscopic brick information ratchet. (c) A cyclic four-state mechanism for the Brownian machine is shown (where W = white, B = black, S = substrate, P = product, and L implies motor bound to S and P) K_b and K_f are equilibrium constants between the black and white stairs. Reproduced with permission.[53] Copyright 2019, The Authors, Published by Springer Nature. (d) Mechanisms of Power stroke (i) elastic relaxation. A fuel processing event (*e.g.*, binding of an ATP or releasing a hydrolysis product, denoted by a lightning symbol): leads to the release of elastic energy. (ii) Conformational transition. Due to the conformational change of the motor, a fuel-processing event leads to a variation in the mechanical element's equilibrium position (denoted by the swinging rod). Before and after the stroke, the motor is not strained; Brownian ratchet: (iii) BR follows the flashing ratchet model; the potential $V_{(x)}$ barrier could change externally by supplying energy and generating a net current. (iv) Rectified diffusion model (based on the concept of information ratchet). Reproduced with permission.[55] Copyright 2019, National Academy of Sciences. (e) A power-harvesting double ratchet motor: fusion of power stroke and Brownian ratchet.[58] Adapted with permission from ref. 89. Copyright 2023, American Chemical Society.

module and undergoes elastic relaxation using the stored potential energy.

2. Chronology of molecular rotary motor development

2.1. Molecular rotors and motors: from switches to rotors

It is possible to convert typical molecular switches to specific molecular machines with rotary functions when they are toggled between more than two states. Often, rotary motion is produced by applying external stimuli, such as light, heat, or electric current. Such switches have molecular components, which change their relative positions (or conformations) in response to these stimuli, producing a change in the overall structure and property of the molecule. These switches, which differ in the directionality for building molecular motors, are explored.[6–8,19] Energy inputs can continuously drive conformations away from chemical equilibrium. Although rotation around a single bond is now well-known, controlling the net directional rotation is highly challenging and elusive. The transitional orientational changes around a single bond axis are an easy trick to convert a switch to a unidirectional rotor.

In the present context, Kelly published a chemically driven system[59] that performs 120° unidirectional rotation around a single covalent bond based on Feynman's 'ratchet-pawl' model in 1999. Nevertheless, the molecular system could not complete a cyclic and fast rotation. Yet, the studies contribute to understanding the design principles of molecular motors. Apart from a single bond, the double bond for molecular switches was exploited to build molecular motors. The inclusion of a sterically bulky unit in a stilbene switch results in helical chirality, which is further explored to develop chiroptical switches.[60] The

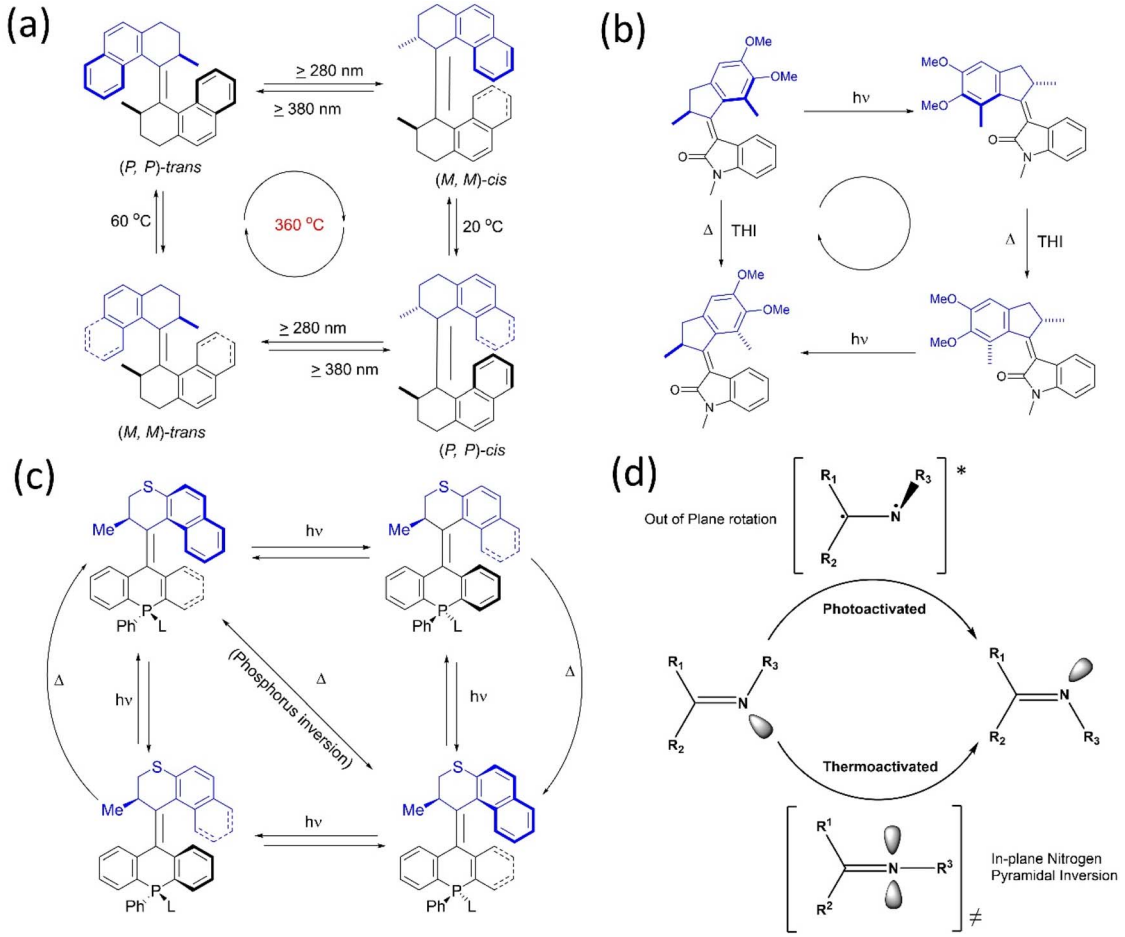

Fig. 2 (a) First light-activated rotary motor.[62] (b) Full 360° rotational cycle of oxindole-based molecular motor.[67] (c) The four-step rotary motion of the phosphine-based molecular motor under photochemical conditions shows a three-step rotary cycle at elevated temperature.[68] (d) Cyclic representation of the isomerization process of the imine rotor that undergoes an *E*–*Z* transition state.[70]

works on light-activated switches laid the foundation for developing light-activated molecular motors.[61] Based on this, Feringa reported the first unidirectional light-activated overcrowded alkene molecular motor in 1999.[62] This motor, featuring two identical halves connected by a double bond, executes 360° unidirectional rotations with four discreet isomerization conformations (Fig. 2a). Both halves contain a chiral point attributed to two energetically uphill *cis–trans* isomerization and two energetically downhill thermal helix inversions (THI), which assist in blocking the reverse rotation because of the steric effect. Therefore, it was a significant step toward building a unidirectional rotary motor for the first time. Afterward, the second and third-generation overcrowded motors were developed, and their properties were investigated extensively.[61,63,64] Feringa's group also extensively worked on various key parameters to upgrade overcrowded alkene rotary motors.[6,8,10,19,65]

Recently, Feringa and coworkers developed a visible light-activated rotary motor based on the *N*-methyloxindole motif synthesized by Knoevenagel condensation.[66] However, due to these motors' low photoisomerization quantum yield, a new oxindole-based motor was developed, which showed a better charge transfer process with increased four-fold photoisomerization (10%) quantum yield (Fig. 2b).[67] In 2020, they developed solely photochemically-driven second-generation motors by the modification of stator parts, possessing four-step photochemically-induced unidirectional motion.[68] A tetrahedral chiral phosphorus stereo element was introduced in the motor's lower half, which could ligate to a gold surface. Moreover, this system could perform unidirectional rotation in three rather than four steps as the chiral phosphorus center undergoes inversion in a thermal environment, which is the conventional isomerization cycle (Fig. 2c). This system could be functionalized to integrate into different surfaces/interfaces to generate smart materials to be applied in various fields.[6,8,10,19,42,65]

Another photoswitch, a C=N bond bearing two asymmetrical motifs, undergoes *E*–*Z* isomerization like an alkene under photochemical and thermal conditions.[69] However, *in silico* studies suggested that an out-of-plane rotation was observed around the C=N asymmetrical bond through a singlet or triplet excited state on exposure to photochemical conditions when *E* to *Z* interconversion occurs (Fig. 2d).[70] On the contrary, the thermal process occurs *via* the inversion of the N motif with

a linear transition state instead of a rotational process. In 2014, Lehn and coworkers confirmed the thermal *N*-inversion path by studying the photothermal *E*/*Z* isomerization of camphorquinone-derived imines.[71] Later on, they described that the chiral imine incorporated rotor shows a four-step rotation instead of a two-step rotation depending on the conformational flexibility of the C-stator part in the rotor[72] as two energetically uphill photochemical isomerization processes, followed by a thermal ring inversion process.

Another type of molecular motor hemithioindigo-based system was designed and developed.[73] Henry Dube and coworkers first reported the motor as mentioned above by including sulfoxide and helical twisting around a C=C bond that performs high speed 360° unidirectional rotation through photoisomerization and thermal helix inversion under visible light.[74] The fast rotation of this motor can slow down by making the system sterically more hindered, providing direct evidence of all four intermediate states of the rotational cycle. In-depth studies of the operational mechanism of the hemithioindigo motor revealed that the unwanted tripled pathway hampered *E*–*Z* isomerization, and the dynamic can be more rapid if the quantum yield of isomerization increases.[75] Notably, thermal ratcheting is essential in converting unstable isomers to stable ones; hence, directional motion is achieved. But this pathway did not proceed at low temperatures, resulting in a motor becoming a light-gated switch. The same group reported another hemithioindigo motor[76] that can perform all the rotational steps more efficiently at low temperatures under a photoreaction (Fig. 3a). These findings by Dube's group provide new insights into the designing principles of light-driven molecular motors.

Inspired by nature, scientists have designed and reported chemically-fueled motors apart from the light-driven molecular motor. In this context, Feringa and coworkers described the directional motion of a motor system around a single covalent bond at the expense of a chemical reaction in four steps.[77] The suitable chemical supply drives the phenyl rotor to rotate relative to a naphthyl stator to afford unidirectional motion in four district steps. However, the requirement of sequential chemical supplies is one of the drawbacks of the autonomous motor; hence, scientists explored and reported better chemically-driven autonomous molecular motors. The same group reported another motor based on an organopalladium motif that provides 360° rotation around a single bond upon supplying chemical fuel.[78] Recently, Feringa's group described a biaryl motor comprised of a carboxylic side chain-integrated aryl rotor that accomplished full cyclic rotation in six steps.[79] Moreover, Leigh and coworkers also reported a chemically driven motor that rotates around the N–C bond,[80] composed of a pyrrole-2-carboxylic acid connected to a different substituent of benzoic acid. Upon the addition of chiral carbodiimide to the diacid system, it is converted into an anhydride system that later settles in a stable conformation (Fig. 3b). Further, the hydrolysis of this intramolecular anhydride motor with an asymmetric catalyst leads to its diacid form. Both reactions were kinetically gate and biased the directional motion, resulting in 360° rotation. Overall, this chemical engine system is an example of a Brownian information ratchet mechanism where the motor performs the task by the consumption of fuels. The authors envision that this first-generation autonomous single-bond rotary motor could be useful in catalytic transformation. These autonomous motors have a high potential to serve as chemical engines.

Frutos and colleagues conceptualized the design of a photoactive unidirectional molecular motor based on chiral hydrogen bond generation.[81] Introducing the hydroxyl and amine group around the double bond of two sides forming hydrogen bonding induced the chiral environment, and isomerization occurs within 1.0 picosecond without forming any intermediate due to the hydrogen bond strength that allows rotation to

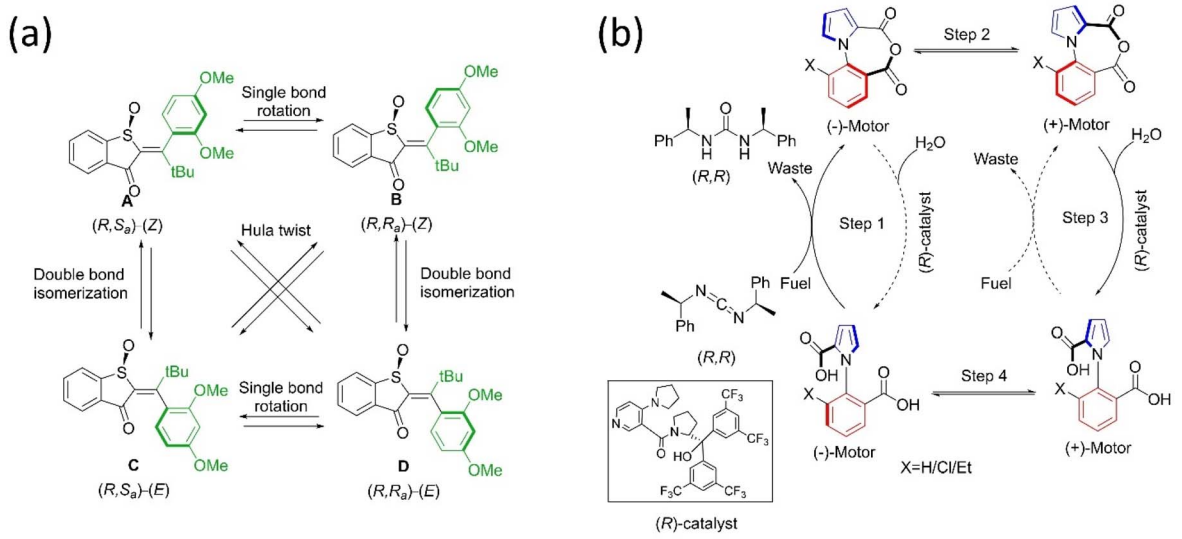

Fig. 3 (a) Molecular structures of hemithioindigo motor with four stable diastereoisomers and their cyclic motion. The "rotors" are colored green.[76] (b) Structure and mechanism of directional rotation in the chemically-fueled motor.[80]

overcome torsion. Several research teams designed other types of molecular motors systems based on azogroup[82] and fulgides.[83] Further improvement by structural modifications is necessary, and the applied molecular motors in various fields are discussed here.

2.2. Dynamics and controls of molecular rotor and motor

One of the main goals of molecular motor engineering is to regulate the mechanical motion that enables measurable outcomes in a controlled manner. An artificial molecular motor should ideally perform practical work reversibly and regulate mechanical motion.[84] Although researchers have successfully built complex molecular rotors and motors, controlling the rotational motion at multistage by tuning different frequencies is yet to be successful, especially other than thermal stimuli. Different techniques are adopted to control the mechanical motion of artificial molecular motors, for instance, cooperative switching, allosteric interaction, pH, and metal ion exchange. Herein, we briefly highlighted a few approaches for controlling dynamic motions with selected examples in the solution and solid phase.

2.2.1. Rotational motion of molecules in solution states. Allosteric effector plays a remarkable role in controlling dynamic motion, which is evident in enzymes where the activity is tuned by it. Feringa's group demonstrated that the rotational speed could be modulated by controlling the steric hindrances of the light-driven rotor using metal ions.[85] The overcrowded alkene motor incorporated with the 4,5-diazafluorenyl unit binds with the metal ions; as a result, the steric hindrance in the fjord region became less (Fig. 4a). Among Zn, Pd, and Pt, the Pt-coordinated molecular motor has a higher rotation speed, followed by Pd. Thus, the dynamic motion of the motor can be modulated from slow to fast into four stages under light stimuli. Schmittel and her group developed a multicomponent rotor to switch off/on the rotor speed associated with catalytic performance based on the allosteric interaction.[86]

All the studies on regulating molecular motion in the range of too slow to ultrafast in various steps reveal that the precise regulation of the dynamic motion of the synthetic molecular

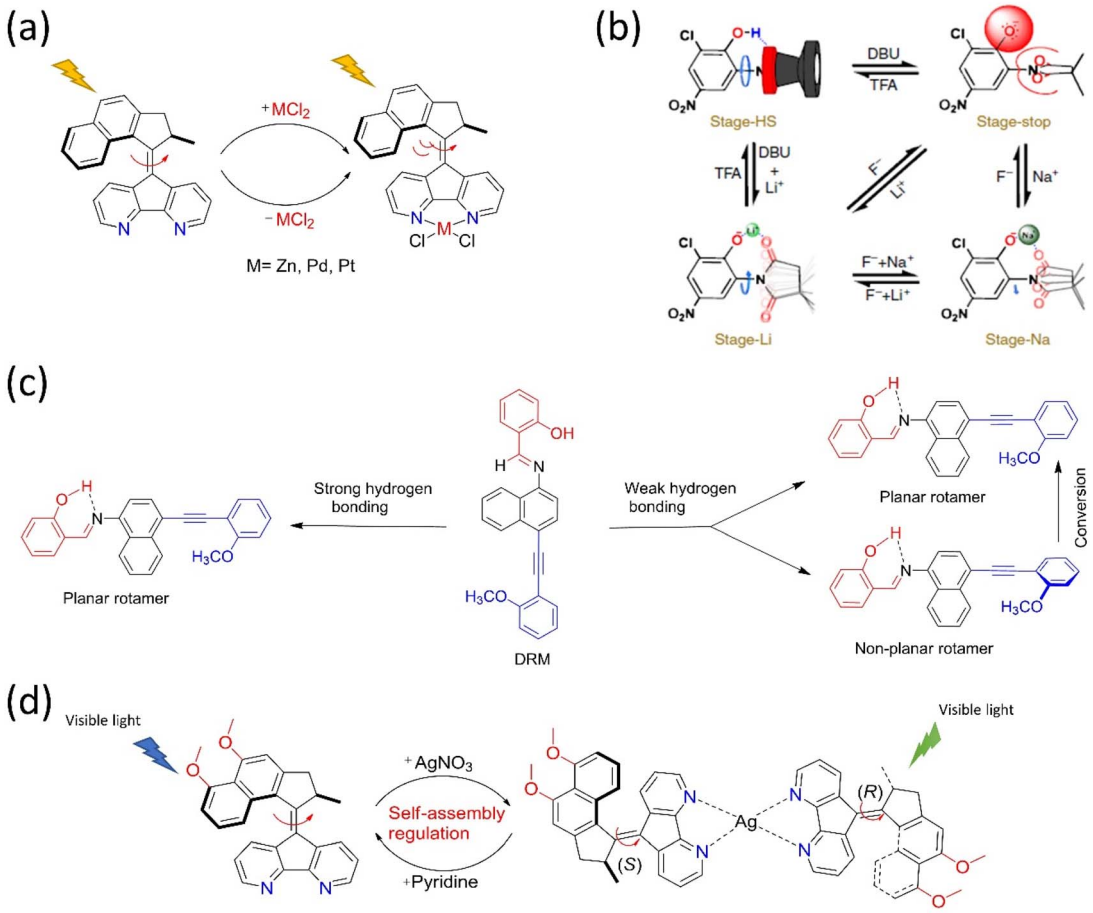

Fig. 4 Approaches for controlling the dynamic motions in molecular motors. (a) Allosteric regulation of the overcrowded alkene-based motor by incorporating Zn, Pd, and Pt metal chlorides under light.[85] (b) Schematic representation of a multistage modulated rotor, in which the four dynamic stages of the rotors are achieved with acid–base and allosteric interaction. Reproduced with permission.[87] Copyright 2018, The Authors, published by Springer Nature. (c) The rotational control of DRM by weak and strong hydrogen bonding. The "BR", "PS", and "AM" moieties are colored blue, black, and red, respectively.[89] (d) Coordination-directed self-assembly of a motorized nanocar.[92]

rotor/motor is still challenging. Wu *et al.* reported the multistage-modulated rotational speed of a molecular rotor that is controlled by pH and metal cations Na^+ and Li^+ cations, which are reversible.[87] This molecular rotor was integrated with succinimide, and phenol possesses a four-stage rotational speed ranging from slow-fast-stop to ultrafast rotational frequency at the same temperature (Fig. 4b). Generally, the OH-group rotates fast. Still, the rotor stops upon deprotonation because of electrostatic repulsion between the carbonyl motifs of succinimide and phenolate anion. The speed could be restored by adding metal ions, which can be monitored reversibly between high speeds to stop employing redox properties. These studies open the way for multistage speed-controlled rotor development by coordinating metal–ligand interactions. In another study, Feringa's rotary motor was modified with a biphenyl system that exhibits slow rotational motion on adding diamine. Consequently, it speeds up as the acid is added to the system.[88] The rotation of a Brownian motor in a double ratchet rotary motor can be controlled by introducing a pawl-like functional unit that can manipulate the electronic distribution of the system. When embedded with the double ratchet motor's PS, an electron-deficient molecule possessing an intramolecular hydrogen bond controls the electronic flow from the BR to the PS (Fig. 4c).[89] The motor operation stops when the intramolecular hydrogen bonding is strong. Thus, this work described that electronic gating could be one strategy to program the double ratchet rotary motors.

The structural modification of the motors by integrating different functional groups is one approach to regulating the motion. For example, the light-gated modulation of the motor's rotation was achieved by introducing a molecular switch in the system. The first multiphotochromic motor was designed based on Feringa's second-generation motor embedded with a DAE photoswitch, which controlled the rotary motion by the light source in a noninvasive manner.[90] The motor becomes operational at 455 nm and stops if the DAE is in a closed state. However, the green light irradiation causes DAE to adopt an open state, allowing the motor to rotate. Pfeifer *et al.* reported a mechanistic pathway to control the rotary motion of a second-generation motor by upgrading it to a push–pull type system by introducing an electron pulling and pushing the group in the lower and upper halves, respectively.[91] Interestingly, this motor follows the function of a motor and a switch based on a polar or apolar environment. Such systems are advantageous if fabricated in different types of frameworks where the function of the motor or switch can be altered as per the situation by varying solvent polarity.

Zeng's group recently developed a molecular nanocar based on the concept of metal-coordination-driven self-assembly, which became operational with green light (Fig. 4d).[92] Here, two chiral molecular motors act as a wheel, self-assembled *via* Ag metal. The dynamics of this motorized system are controlled by adding pyridine, which breaks down the system into two individual motors. This triplet–triplet intramolecular charge transfer sensitization and push–pull features of the nanocar make the system operational at 500 nm, whereas the individual motor is functional in the blue region. Moreover, this is the first example of coordination directed self-assembly to initiate motor conversion into a nanocar and easily dismantled by adding chemical stimuli to realize the goal of metal-driven transportation and release.

2.2.2. Rotational motion of molecules on solid surface. The research in the molecular machine domain gradually shifted from the solution phase to the solid state, and the regulation of the motion in a solid interface is challenging. Recently, a few groups precisely reported the control over the rotational speed in the crystalline phase.[93,94] For instance, Comotti and coworkers described the modulation of the rotational frequency of the ultrafast molecular rotors in crystalline 3D porous materials.[95,96] In a published report, Comotti described a nanoporous material containing molecular rotors based on a biphenyl molecule that can rotate around a single bond axis. The guest molecule's inclusion in the nanopores modulated the rotational dynamics of the molecular rotors from slow to ultrafast.[95] The removal and inclusion of suitable guest molecules enables finely tuning the rotational dynamics reversibly. Hence, a suitable choice of guest molecule(s) that act as brakes allows the regulation of a wide range of rotational motions at specific temperatures. Further investigation with a new rotor with the *p*-phenylene moiety revealed that the rotational motion could be actively regulated in response to guests as the temperature is increased, the rotors spin ever faster, approaching free-rotational diffusion at 550 K.[96] Moreover, the addition of small guest molecules such as iodine can cause a significant increase in the rotational barrier of the rotor, thus slowing down the rate of rotation. This effect is attributed to the steric hindrance of the guest molecules, which interferes with the free rotation of the propeller. In addition, the rotational dynamics of the rotor were highly dependent on the size and shape of the pores in the organosilica matrix. For example, the rotation rate was slower in smaller pores due to the rotor blades' increased steric hindrance and restricted motion. These studies provide insights into how molecular rotors can be modulated and controlled in a nanoporous matrix, which has important implications for developing molecular machines and nanotechnology applications. Hence, the rotation is facilitated by the freedom of motion of the rotor within the nanoporous material, which differs from Feringa's unidirectional motors that need light as an external stimulus.

The same group reported a porous molecular crystal comprising rotors linked through charge-assisted hydrogen bonds, and their dynamic was switchable through gas adsorption/desorption.[97] In another report, they developed a metal–organic framework (MOF) fabricated with a rotor that exhibits fast rotation.[98] Herein, a zinc-based framework was composed of a rigid bicyclopentane–dicarboxylate linker where the bicyclic unit serves as the rotor. The carboxylic stator motif aligned perpendicularly in the cubic unit of zinc-based metal frameworks enables ultrafast rotation, which is attributed to high torsional flexibility. This aliphatic linker achieved unidirectional rotation with a speed of 10^{10} Hz even at temperatures below 2 K. This system described rotary motion at low temperatures by continuous unhindered molecular wheel rotation for several turns. This could be attributed to minimized thermal energy as the temperature becomes low. Although molecular motion usually freezes at low

temperatures, no such hindrance was observed in this fast rotor, exhibiting low torsional barriers compared to their thermal energy. Thus, these rotors could be implemented for working in low-temperature ranges. Horike and his group reported another type of work in which the precise regulation of the rotational motion of a rotor in the crystalline phase could be achieved using a solid-solution approach.[99] The variation of solid/solution ratios would modulate the volume of cells in porous materials, which led to changes in the rotational barrier for pillar rotors; therefore, rotational frequency control requires no thermal stimuli. However, the speed could be mainly regulated from ultrafast to fast; thus, the challenges still need to be addressed.

2.3. Exploring working motor-based device prototypes

Macroscopic machines assemble many complementary parts to perform a specific task.[100] A molecular machine is capable of complicated operations comparable to a macrodevice, except that the molecule's mode of operation differs and the device's power source is irrelevant. Top-down approaches have delivered many solid-state miniaturized devices. Although targeting sustainable molecular level precision, this has not gone well. The concept of miniaturization of components is exploited by the bottom-up strategy that offers to manipulate the molecules in the nano-domain.[101] The development of supramolecular chemistry plays a crucial role, allowing molecular machines to build smart materials and supramolecular architecture-based devices, hence offering practically limitless potential.[102] Researchers attempt to produce smaller semiconductors with photolithographic and chemical etching techniques. The semiconductor devices from 65 nm to 14 nm chip have been developed, and now the 7–2 nm chip has been explored.[103–105] However, there are a few hurdles associated with the molecular level device design, such as the Fermi energy level of the electrode, which should be appropriately aligned with the molecular orbital of the molecules to develop a molecular transistor.[106] Scientists have attempted to develop a single molecular device that can overcome the limitation of Moore's law.[107] The significance and development of single-molecule electronics are outlined owing to the limitation of Si-based devices.[108] Several methods have been developed to study single molecular electronic devices in the last few decades. Molecular motors/switches can exhibit different states beneficial to developing high-density molecular electronics. Tour and his team have recently developed a chip integrating a single molecule in a circuit, resulting in a programmable biosensor.[109] This semiconductor chip consists of a scalable sensor array architecture, and an electric meter is integrated with each array that records the current flow through the molecular wire. The desired molecule is connected to the wire *via* a conjugation site that offers a real-time electronic readout of molecular interactions of the probe.

3. The use of molecular rotors and motors

3.1. Uses in energy conversion harvesting and transfer

The ability of motor proteins to transform chemical energy into mechanical motion represents energy conversion and storage in molecules. Because the motor protein has the additional property of dynamic density of states (DOS), the mechanical movements of a molecular motor may lead to dynamic switching states in a device. It is a significant advantage for using such molecules to advance molecular electronics, energy transfer, and energy harvesting from available solar, thermal, or any other form of energy. For this purpose, different molecular systems are engineered with the semiconducting surface, resulting in an energy harvesting device. For example, Feringa's group developed a visible light-driven motor integrated MOF, where two components are palladium-coordinated porphyrin and bipyridyl-functionalized overcrowded motor.[110] The porphyrin moiety absorbs visible light energy to run the motor by transferring the energy to the motor struts (Fig. 5a). Irrespective of the solution and solid state, this advanced photochemical process of the motor was observed to be unchanged. Thus, the system functions as an energy harvesting unit where the photon energy is utilized to result in nanomechanical motion within the nanocage of MOF. Such a MOF-nanopocket is useful in improving the catalytic reaction kinetics.[111] In the context of the energy transfer process, Bojinov and his group synthesized a multicomponent light-harvesting molecular rotor that can also sense pH and viscosity.[112] The system comprises a switch, rotor, and a light-harvesting motif that transports up to 99% energy through a fluorescence resonance-energy transfer process. Moreover, a radiofrequency-guided dual ratchet motor can convert available thermal energy to power under applied bias when integrated on a highly oriented pyrolytic graphite (HOPG) surface (Fig. 5b). The Brownian rotor mechanism of the motors uses available thermal noise, and the chip harvests an excess power than the input bias.[58] The system can harvest noise when dipped in a suitable solvent and exposed to electromagnetic radiation. Thus, Brownian rotors absorb noise (kT), and the produced thermal fluctuation in diffused solvent molecules leads to energy conversion.

In 2015, a new photoswitch hemithioindigo[113] exhibited superior photophysical properties and was used to build a molecular motor.[114] Herein, the sunlight energy was supplied to the motor to perform the unidirectional motion. Henry Dube and his group reported several hemithioindigo motor systems[115,116] that displayed an efficient visible light-induced photo-isomerization process in the last few years. These design strategies for constructing green molecular motors could be used as power sources or as active materials in solar cells for better solar energy conversion.[117,118] The molecular motors are coupled with the polymeric chain to harness the energy used to perform mechanical work at a macroscopic level. Giuseppone and coworkers have demonstrated that the contraction of the gel made of overcrowded alkene motor is integrated with polymers owing to the dynamic motion of the rotary motor.[119] Thus, the rotational motion of the motor stores the light energy in the form of potential energy in the polymer. However, the stored energy cannot be accomplished again owing to the irreversibility of braiding the polymer under light. Thereby, the group has introduced a diarylethene switch that serves as a modulator in the gel system that assists in overcoming the abovementioned issue.[120] These molecular motors are eligible for energy harvesting or

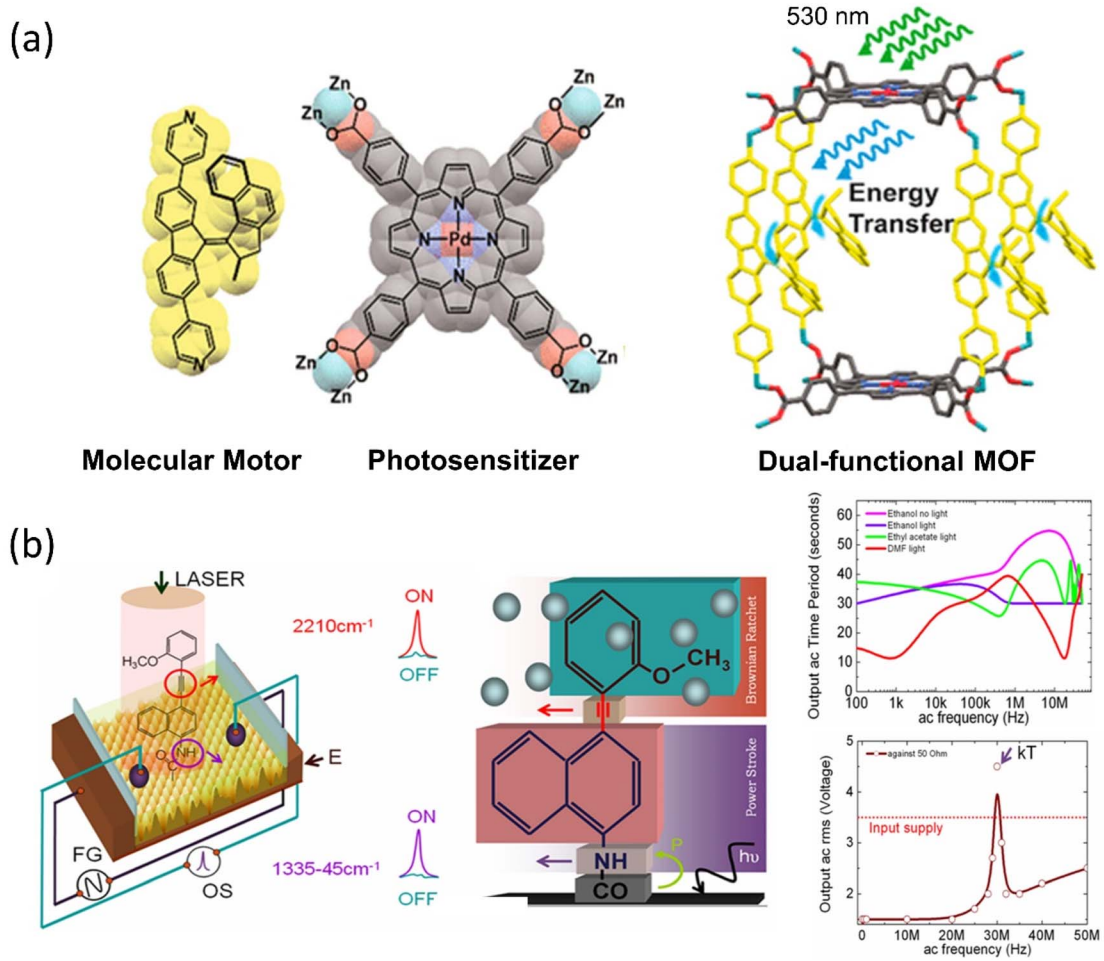

Fig. 5 (a) Design and molecular structure of visible light-driven molecular motors in MOF. Reproduced with permission.[110] Copyright 2020, American Chemical Society. (b) The dual rachet motor on the HOPG chip and the graph of power production as a function of AC applied frequency. Reproduced with permission.[58] Copyright 2020, American Chemical Society.

storage, which could be used for future purposes; however, more challenges exist in developing a power harvesting device.

3.2. Possible uses of shaft-based rotary motors as wheel and propeller

Tour developed the first nanocar bears wheel-like C_{60} fullerenes and various molecular motor-based vehicles that show collective motion on the solid surface, for instance, nanotrucks, carborane nanocars, and light-powered nanocars.[121–123] In 2016, Grill *et al.* showed the translational motion of a three-wheeler nanocar based on the rotary motions from two adamantane moieties and a Feringa motor as a third wheel.[124] The nanocar was analyzed on the Cu(111) surface by STM, illuminating a 355 nm light for photoisomerization and then 161 K temperature for helix inversion (Fig. 6a).[125] Thermal-induced helix inversion was crucial as these steps led to the nanocar to perform lateral translational motion. The mean-squared displacement of the motor without light was 3.37 ± 1.00 nm^2, increasing to 10.48 ± 4.10 nm^2 under light exposure of the mean squared displacement of the light. All these reported nanocars were investigated at the molecular level under STM, which requires a conducting surface. Taking it one step further, the group incorporated the nanocar with a fluorescent dye, which could be studied in single-molecule fluorescence microscopy on a nonconducting glass surface. Feringa's group upgraded the various motorized nanocars by incorporating BODIPY in different positions to control the net directional motion.[126,127]

Although, owing to higher THI, the rotational rate of the motor decreases compared to the motor without BODIPY, which isomerized up to 91%. The structural redesign of the nanocar addressed this problem as the system avoids the energy transfer process, which lessens the photoisomerization process. In addition, the motor with more photostable BODIPY dye compared to the least stable Cy5 dye is a better choice to study on the glass-air surface.[128,129] Later, with these structural advantages, a line scan imaging protocol was developed that facilitates the four-wheeled BODIPY-functionalized nanocars gliding in a quasi-random 2D manner on the glass surface. Nanocar 1 shows better performance as it is able to maintain a linear trajectory and move on the air-glass interface with

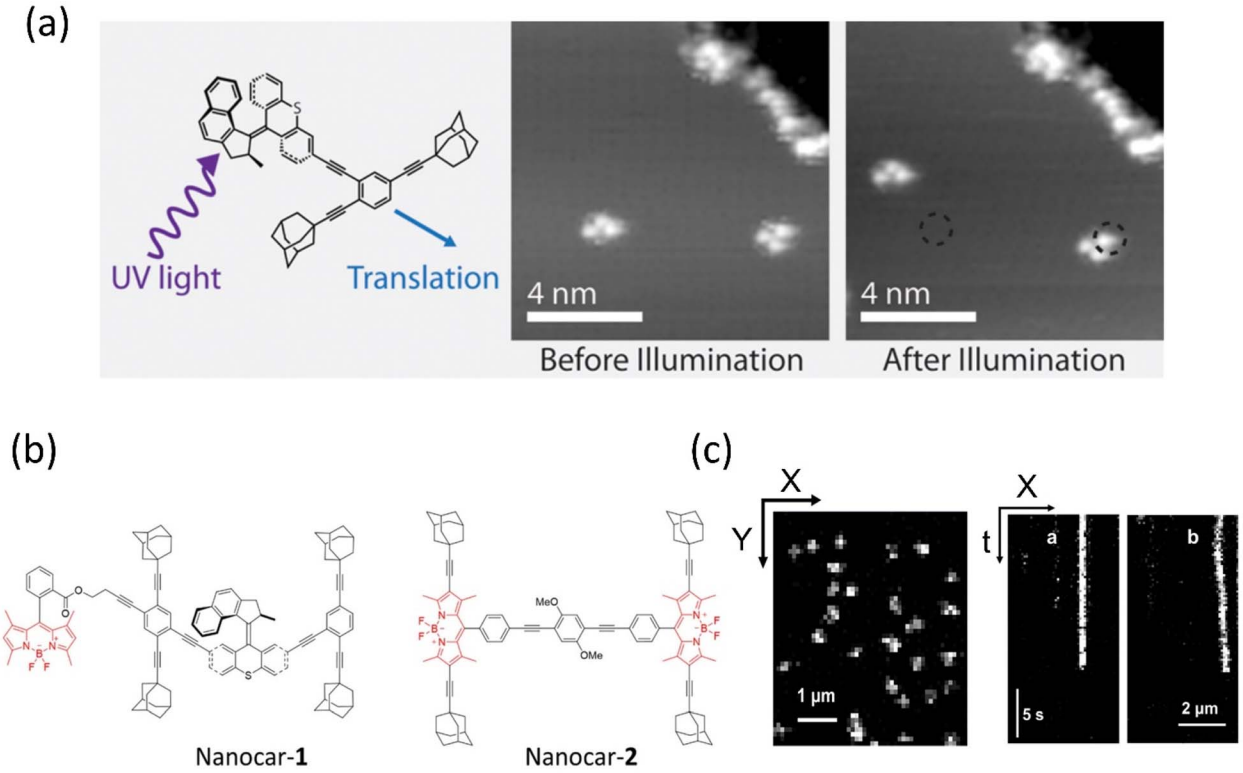

Fig. 6 (a) Molecular structure of light-activated motorized nanocar. The photoinduced motion of a molecular rotor on Cu(111) surface at 161 K. Reproduced with permission.[125] Copyright 2016, American Chemical Society. Line-scan imaging protocol (b) nanocar 1 & 2 equipped with adamantane wheels and BODIPY. (c) Conventional 2D photograph of nanocar 2 on the air-glass interface. (a and b) The line-scan images of nanocars 1 and 2 where nanocar 2 is in motion while nanocar 1 is immobilized. Reproduced with permission.[126] Copyright 2018, American Chemical Society.

a quasi-random 2D diffusion mode (Fig. 6b and c).[126] This fast-line scanning imaging protocol accurately estimates the diffusion coefficient of molecules. In 2017, Tour, Grill, and coworkers reported the surface rolling motion of the nanocar,[130] where the effect of the dipole moment upon the electric field was described. The nanocar was comprised of electron push–pull groups in an aryl ring, namely, dimethylamine and $-NO_2$ group, along with two adamantanes as a wheel. The dipolar nanocar was manipulated with the electric energy in an STM that exploited the dipole molecules and induced the unidirectional motion. These systems were highly oriented on the Ag surface with high precision due to the dipole moment of a nitro moiety that interacts with the surface, causing translation motion (Fig. 7a and b). Thus, the nanocar's design and surface rolling properties with various surfaces to afford better directional property is challenging but essential.[131,132] Jacobson *et al.* described Feringa-developed motor adsorption on the TiO_2 (110) surface trapped by the –OH group, resulting in a charge transfer process.[133] These outcomes could assist in developing motor-incorporated organic–inorganic nanodevice for a wide range of trafficking on the nanosurfaces.

Metal ions have been observed to act as a controller of molecular motions due to their reversible ligand binding nature, ability to change coordination geometry, ligand exchange, and reactivity to external stimuli. Metal-centered molecular machines capable of switching rotary motion either through metallation/demetallation or by changing the coordination number of the metal center have been facilitated by such properties, albeit the latter remains mainly unexplored. For instance, Ube *et al.* reported a Pt(II)-centered molecular rotary gear constructed using two azaphosphatriptycenes as rotators and one Pt(II) ion as a stator (Fig. 7c).[134] The molecular rotary motion transmitter demonstrated control of engagement and disengagement in the rotor. It was in accordance with the isomerization of the *cis*- and *trans*-forms initiated by photochemical and thermal conditions. The repeatable isomerization between a disengaged *trans*-form and an engaged *cis*-form was found to be reversibly navigated by heat and photoirradiation of ultraviolet light. They suggested that such mechanical switching based on *cis–trans* isomerization of the Pt(II) ion center operated by photo and thermal motion would yield a selector switch for more complicated molecular machines.

In 2017, they reported another gear system consisting of six triptycene gear units in a circular arrangement around a benzene ring (Fig. 7d)[135] through an ethynyl linker. These six triptycene gears had a close engagement; coordinating a bulky RuCp* complex to any of the six gears, they observed high restriction on the overall movement of the six gears within the molecule, although the movement was not completely stopped. This RuCp*-bound multigear molecule is chiral; thus, despite

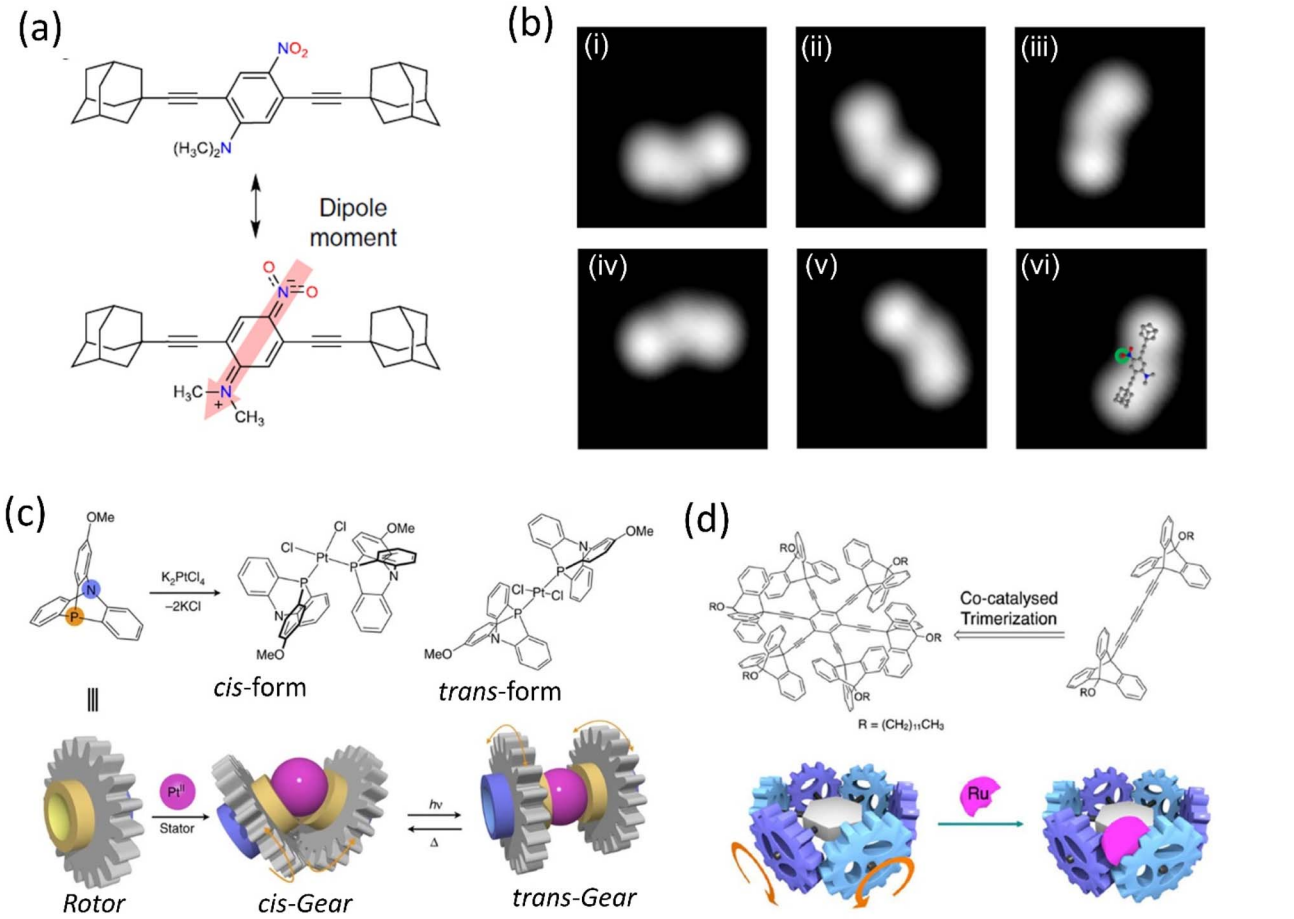

Fig. 7 (a) Chemical structure of polar motor. (b) (i)–(vi) STM images of the molecule showing clockwise rotation upon applied voltage pulse. Reproduced with permission.[130] Copyright 2019, The Authors, published by Springer Nature. (c) Schematic representation of a Pt^{II}-centered molecular gear exhibiting *cis–trans* isomers could be achieved upon ultraviolet irradiation at 360 nm and heating. Reproduced with permission.[134] Copyright 2017, The Authors, published by Springer nature. (d) Ru-centered sextupled triptycene gear. Reproduced with permission.[135] Copyright 2017, American Chemical Society.

having nondirectional motion, the rotational rates of the different gears from one another were different. This multigear molecule provides a structural basis for the long-distance transmission of molecular gear systems containing an on/off function. Recently, Asato *et al.* developed an electron-triggered Ru-based molecular motor integrated photoresponsive brake and studied dynamic motion on the surface employing light.[136] This dual responsive system shows clockwise and anticlockwise directions. Recently, Dube's group reported the photogearing motion of a hemithioindigo-based molecular gear that can transfer the rotational motion, *i.e.*, the isomerization around the double bond results in 180° rotation.[137] As a result, the associated single bond with the double bond undergoes 120° rotation. This photogearing process at the nanoscale can be correlated with the bevel-gear system. Moreover, light as an external stimulus for gearing motion before a thermal-driven motion has several advantages.

The gear and axle development would improve the molecular motor's design, enabling better control of the nanorobotics' movement.[138–140] Hla's group designed a molecule propeller consisting of three molecular blades[141] connected to a ruthenium atom in a facial mode connected to the stator. STM studies clearly showed each molecular propeller's motion on applying electrical voltage. The system was grafted into the Au surface and manipulated in STM by different techniques to analyze the unidirectional rotation. Moreover, the 2D nature of the gold surface and ratchet shape gear in the system introduces the chirality that initiates 360° rotation that splits into 15 steps when the system is energized in STM. The generation of chirality by synchronizing the ratchet mechanism is the crucial factor for the movement, and this concept could potentially develop a wide range of applications.

3.3. Possible use of motor in cargo delivery

Amphiphilic molecules could be arranged from the nanoscale to the macroscopic domain through 3D supramolecular assembly on applying the external stimuli. Tian and coworkers described the preparation of a tetraethylene glycol-functionalized amphiphile cargo based on an overcrowded alkene system (OAS) capable of forming well-defined vesicles in

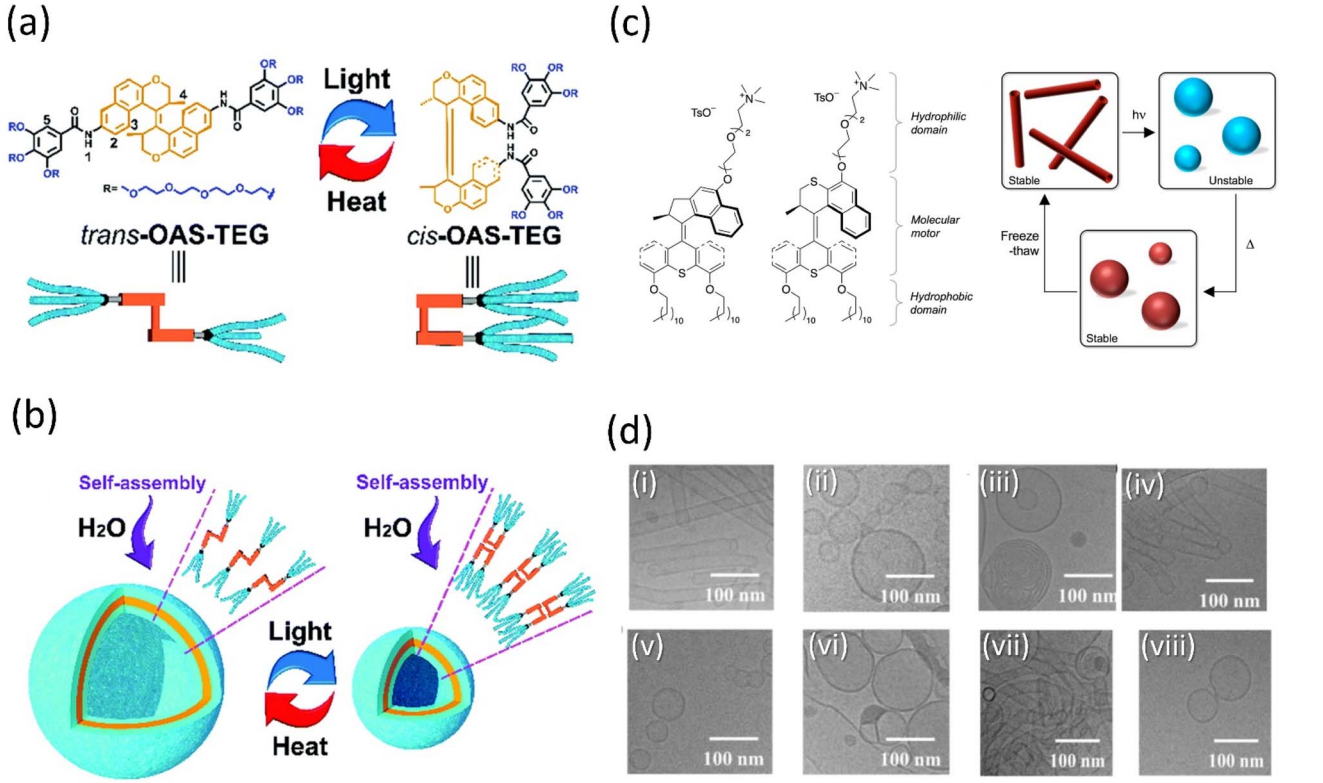

Fig. 8 (a) Interconversion of OAS-TEG upon light and thermal irradiation. (b) Self-assembly of OAS-TEG in an aqueous medium to form vesicles. Reproduced with permission.[142] Copyright 2016, Royal Society of Chemistry. (c) Amphiphilic molecular motors 1 (fast) and 2 (slow) and their change in aggregation upon the isomerization of self-assembled molecular motor constituent. (d) Reversible isomerization of motor 2 and DOPC (1 : 1) (i) starting point, (ii) after irradiation, (iii) after heating, (iv) after three freeze–thaw cycles, (v) after irradiation, (vi) after heating, (vii) after three freeze–thaw cycles, (viii) after irradiation. Reproduced with permission.[143] Copyright 2011, Springer Nature.

a water-based solution (Fig. 8a and b).[142] When the vesicles were exposed to light, the nanocontainer contracted due to the isomerization of alkene between its *cis*- and *trans*-states. As a result, the vehicle's internal volume will alter, allowing them to wrap cargo in its cavities and release it depending on the situation. Examining the ability of vesicles to encapsulate indicates that under light, calcein-loaded *trans*-vesicles release at a high pace, as measured by fluorescence intensity. Thus, these photoresponsive vesicle-based smart nanocontainers could facilitate the construction of remote drug delivery systems in the future, which may further inspire the development of motor-based vesicles.

The complex yet fascinating self-assembled polymeric molecules in nature have inspired Feringa and his group to put forward a novel concept of creating a unique molecular motor system in water that is amphiphilic and self-assembles into well-defined supramolecular nanotubes based on their earlier report.[143] These self-assembled polymers changed their morphologies back and forth when exposed to external stimuli as the motor isomerized. It was the first example of a molecular rotary motor that self-assembled in an aqueous medium without losing its functionality (Fig. 8c and d), alternating the photo and thermally-induced steps, an isomerization process-controlled reshuffling between the nanotubes and vesicles. Thus, it provided access to the new future of water-soluble motors and opened the pathway to produce highly progressive and dynamic artificial nanosystems in water. Although the cargo activity of the aforementioned self-assembled vesicles and nanotubes is not reported, owing to their aqueous solubility, they may develop certain properties that would help cargo delivery.

Chen and coworkers reported that dual light controls dynamic supramolecular assemblies comprised of Feringa's first-generation motor, which bears both hydrophobic and hydrophilic chains and exhibits controlled foaming abilities in water at the macroscopic level.[144] The design was such that *trans*-isomer form with lower packing parameters than the *cis*-isomer displays precise control over the aggregation properties (Fig. 9a and b). The system exhibits four states that systematically control the geometrical structure from the nanodomain to the macroscopic domain as two distinguishable worm-like micelles, resulting from stable *trans*-isomers and stable *cis*-isomers associated with vesicles. At the same time, unstable isomers exhibit a mixture of geometries. The reversible foaming-property switching could be achieved until ten cycles upon periodic light and heat irradiation. The further exploitation of this field with a dynamic system will unveil other possibilities.

To maintain the physiological functionalities of living cells, the transportation of ions across the lipid membranes is

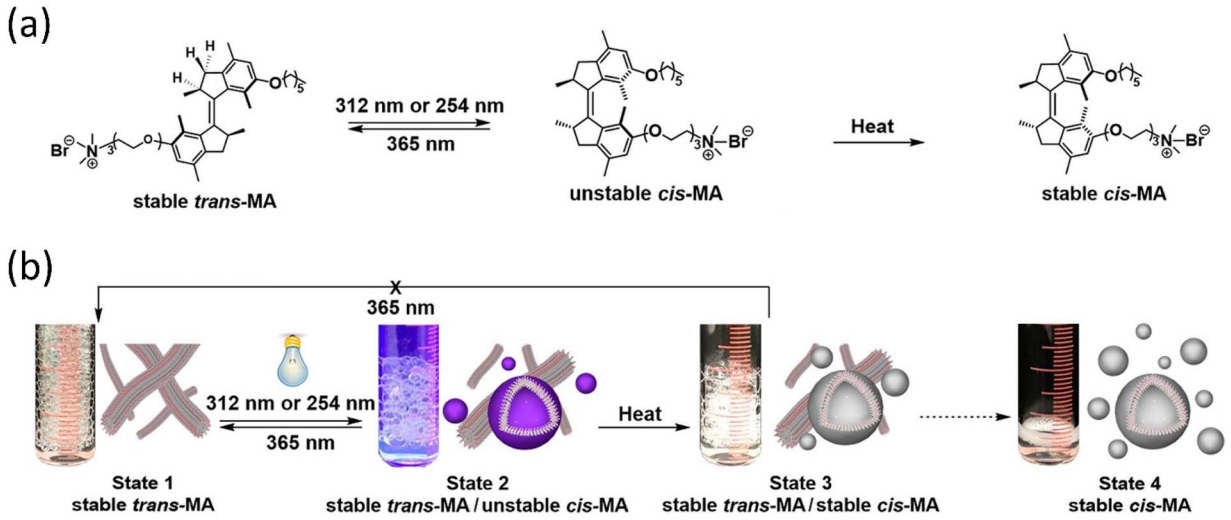

Fig. 9 (a) Light-responsive molecular motor amphiphile (MA) and its reversible photoisomerization process. (b) The alteration in visible macroscopic foaming processes brought structural changes in the supramolecular assembly. Stable synthetically purified *cis*-MA is used to create state 4. Reproduced with permission.[144] Copyright 2020, American Chemical Society.

necessary. Nature carried out these cargo tasks selectively employing biological motors under chaotic environments with chemical fuel or light absorption. However, mimicking such a natural system to develop synthetic molecular motors are highly challenging and desirable at the same time. Wen and colleagues reported an artificial motor system embedded with azobenzene (AB) that transports cyclodextrin molecules across the synthetic nanochannels upon exposure to light.[145] Here, the light energy initiated the rotational inversion of the AB molecular motor along with hydrophobicity and reversible photoreaction of the system, enabling the transport of the molecules across the nanochannels. Recently, Giuseppone and coworkers synthesized the light-powered hydrophobic rotary motor that integrated with two macrocycles and investigated their ion transport properties in a phospholipid membrane.[146,147] The motor system was also embedded with a urea motif that forms a hydrogen bond, which induces the supramolecular self-assembled with the phospholipid membrane. The crown ether macrocycle can encapsulate the alkali metal ion. The fluorescence assays and patch clamp investigations revealed ion channel formation with the rotary motors system. Furthermore, the transportation could be enhanced up to 400% on exposure to UV light, which could be attributed to the photoactuation of the rotary motor that provides sufficient energy to the passage of the alkali metal along the artificial pore.

3.4. Biomedical uses of rotors and motors

Tamaoki and colleagues presented a peptide-integrated AB machine that disables the function of the kinesin microtubule.[148] The system comprises an electron-withdrawing and an electron-releasing group to decrease the lifetime of the *cis*-isomer by shifting the π–π^* band toward the visible region. The transformation of the machinery mentioned above disables the kinesin microtube's motility without hampering the other filaments, but the *cis*-form enables the movements. As a result of the rapid thermal relaxation from *cis*-to *trans*-interconversion, the machine was efficiently functioning in a single wavelength to control kinesin movement. This push–pull machinery is an excellent example of engineering in developing a synthetic machine incorporating biomolecular motors for better results.

It is reported that the double ratchet motors were used in a nanoplatform to develop higher-level nanomachines (PCMS and PCBM).[149–151] PCMS nanomachine comprised of PAMAM dendrimer as matrix molecules has been found to target cancer cells specifically. The 3G (400 MHz–3 GHz) mobile radiation was used to activate it, which sensed the microsatellite instability and disintegrated the nucleic acids through the energy transfer process by the motors.[149] The working principle of PCMS was showed that when the GHz signal was shone on PCMS, it generated oscillation frequencies matching the microsatellite instability of cancer cells. On the other hand, PCMS resonance oscillation could also be matched to Alzheimer-related beta plaques at room temperature (Fig. 10a–c). This standalone system performed its job as a purely mechanical drug *via* a triangular energy transmission path (S → C → M); therefore, the physical mode of interaction of PCMS could avoid or minimize the side effects compared to chemical interaction. Further, the PCBM crypto nanobot resonance drug was built based on the information from the motor-functionalized dendritic system and investigated the various parameters, which will not be affected by proteolytic enzymes.[151] This cryptosystem comprises a double ratchet motor and streptavidin marker protein-specific biotin (Fig. 10d). The study of PCMS and PCBM demonstrated the possibility of replacing generic cancer medications as well as paving the way for developing a more dynamic system with a novel molecular rotor that might be used in the medical area to produce physical and mechanical drugs.

Overcrowded alkene-based motors are primarily employed in biology and show remarkable outcomes. Tour's group created

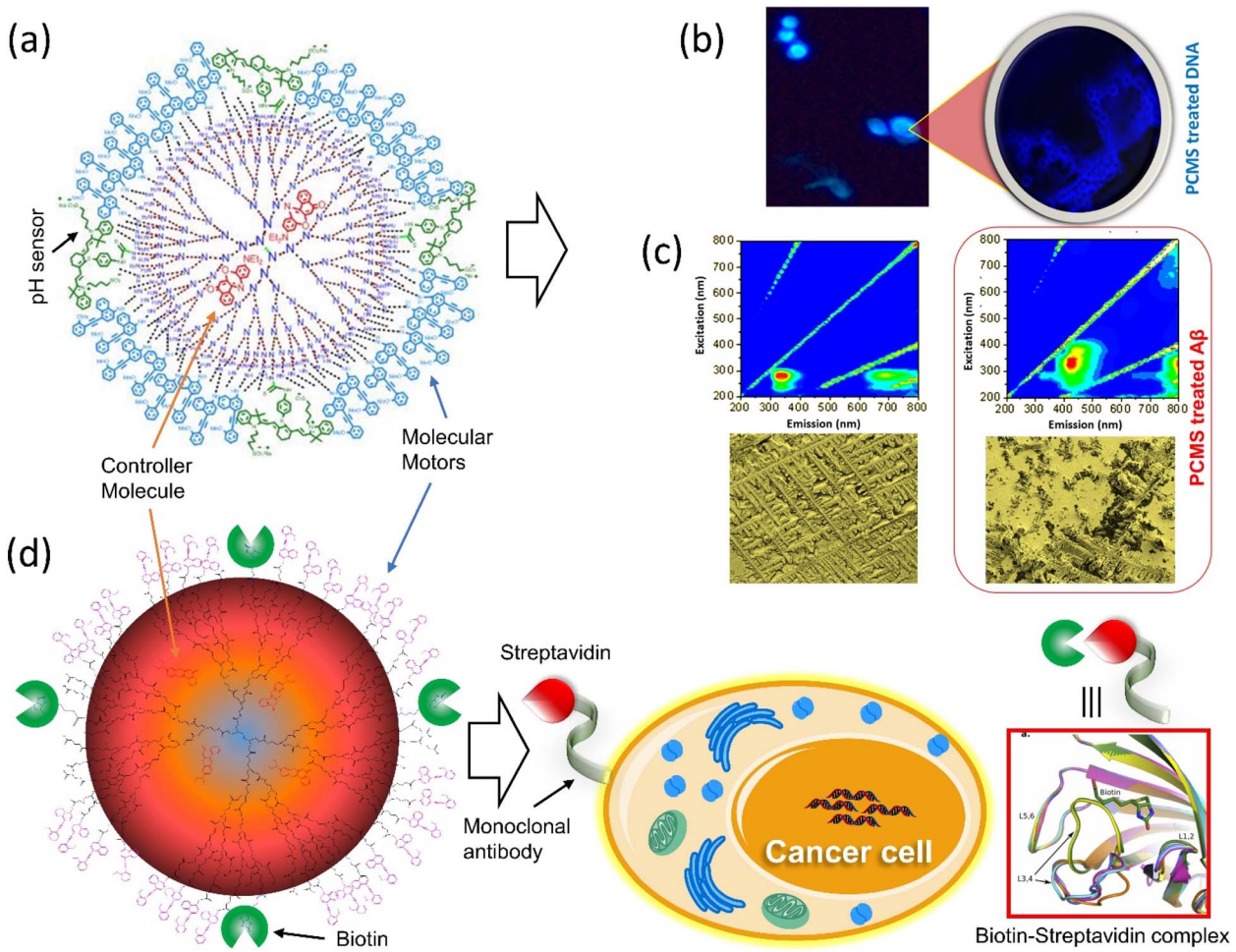

Fig. 10 Dual ratchet motorized PCMS. (a) Molecular structure of PCMS. (b) The nanomechanical action of PCMS destroys cancer cells and (c) the nanomechanical action of PCMS disintegrates αβ-plaques.[149] (d) The target-specific crypto nanoassembly system.[151]

light-driven versions of molecular machines that can pierce biological membranes and use them for target-specific cell tracking by tagging fluorophore-integrated motors, peptide-linked motors, *etc.*[152] The group discovered that a biocompatible-functionalized light-activated Feringa's motor could adsorb onto lipid bilayers and when activated, drill into the cell membranes. They demonstrated the *in vitro* applications of the simple to a target-specific molecular machine that induces necrosis, such as human prostate cancer cells targeting motor functionalized SNTRVAP-peptide specific to the 78 kDa glucose-regulated protein (GRP78), were developed. Notably, this activated motor enhances necrosis by 40%, and a simple untargeted motor fastens necrosis by 50% compared to the necrosis induced by solely UV light (Fig. 11). These findings confirmed that molecular machines could function at the cellular level. However, the disadvantage of requiring harmful UV light to activate the motors must be addressed. Later, the same group described how near-infrared–triggered two-photon excitation (2PE)–activated molecular machines that could drill through the cell membrane to destroy cancer cells,[153] which is superior in the *in vitro* application compared to an earlier report. These molecular machines could make targets specific to cells by tagging the specific peptide chain or antibody, possibly potential cancer cells (Fig. 12a and b). The same group tagged fluorescent dye Cy-5 with the machine for monitoring synthetic bilayer vesicles. They studied cell death in different cells using untargeted and targeted nanomachines, whereas the untargeted nanomachine initiated necrosis at a much higher rate than the UV-activated necrosis. A similar observation was reported for the SNTRVAP peptide-functionalized motor. The MCF-7–targeted peptide sequence DMPGTVLP functionalized with the machine displayed necrosis at the rate of 63% within 3 min in the *in vitro* test. However, this method requires that the penetration level of cells be limited.

In 2019, the same group upgraded the nanomotor that destroyed pancreatic cancer cells upon activation with 405 nm light.[154] As structural modifications on the motors change the rotary rate, consequently (Fig. 12c and d), fast rotor causes cell death within 5 min, whereas the slow and medium motors need 20–15 min. These mechanical motors inhibit the production of the reactive oxygen species responsible for cancer cell death. However, these systems fail to penetrate deeper into the tumor yet can treat diseases such as shallow oral, gastrointestinal, and genitourinary cancers. Moreover, the fast mots among these

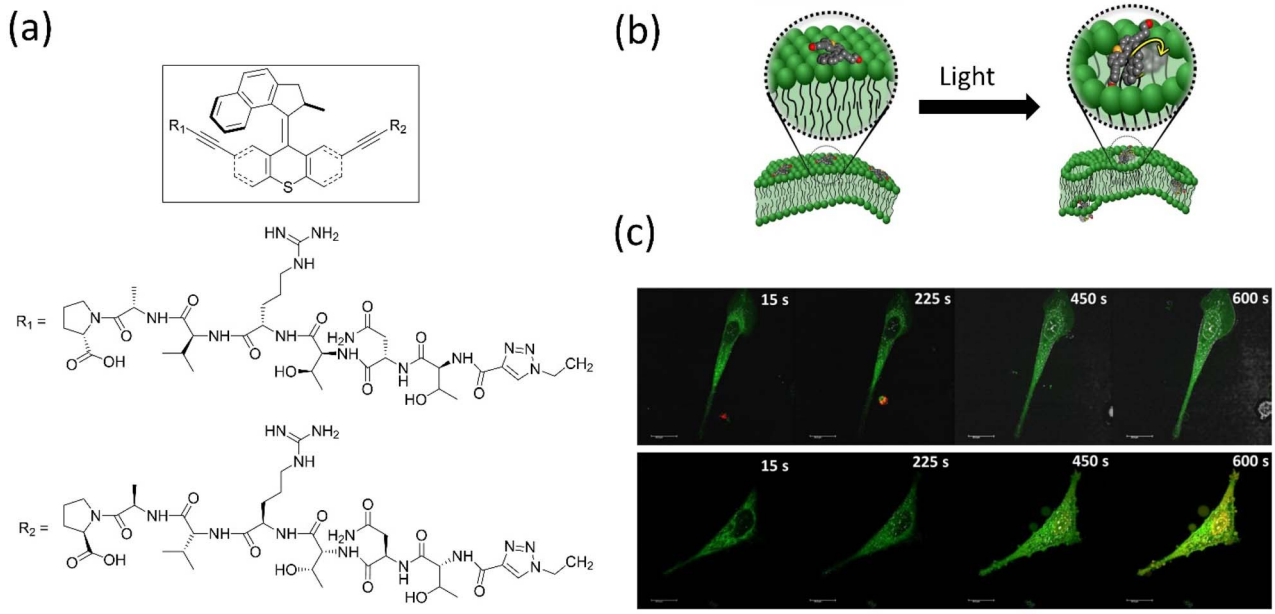

Fig. 11 (a) Structure of molecular motor along with the peptide SNTRVAP sequence. (b) A representative diagram of a molecular machine that opens a cell membrane upon light irradiation. (c) Photographs showing the action of a SNTRVAP-functionalized molecular motor on PC-3 cell. Necrosis induced by the motor upon light exposure within a time interval is presented. The scale of all photographs is 20 μm. Reproduced with permission.[152] Copyright 2017, Springer Nature.

motors are able to raise the mortality rate in *C. elegans* by 70% and in daphnia by 100% and are also potent in destroying the prokaryotic cell, eukaryotic cell membrane, and many physiological functions of multicellular eukaryotes *in vivo* and *in vitro*.[155] Such a system could treat diseases such as skin cancer, cosmetic application, and parasite controls.

Inspired by actin filaments and myosin, Zheng *et al.* reported a molecular machine incorporated with two triethylene glycol chain polymers that can exert force at the cellular level equivalent to 12 kT and induce mechanotransduction processes.[156] The light-induced rotation of the motor is braided into the polymer chains to minimize the receptor-interface linkage. Consequently, a mechanical force is applied to the cell membrane receptor, which causes mechanotransduction. These works were related to force-dependent cellular works such as T-cell activation and focal adhesion (FA) maturation. An alternative approach to achieve visible light-driven rotation of these molecules is to take advantage of intramolecular or intermolecular sensitization through triplet energy transfer from a second chromophore. Pfeifer *et al.* developed a NIR range-activated molecular motor integrated with a two-photon absorption (2PA) sensitizer dye.[157] The motor was activated with low-intensity NIR light *via* the resonance energy transfer process, which is more convenient in biological studies, such as *in vivo* studies. NIR light first activated the sensitizer, conveying this energy to the rotor for rotation. These findings lead to the development three-photon activator systems that may hold more efficiency and be more compatible with the environment. Stimuli-responsive transmembrane transport proteins play an important role in biological systems, and defects in them cause serious diseases. Various transporters are developed, yet stimuli-responsive materials are highly desirable.

Wezenberg and coworkers developed an anion-binding stiff stilbene system modulated by light.[158] These anion receptors are modified based on their previous work,[159] where the system shows a high affinity toward acetate and dihydrogen phosphate.[160] The *Z*-isomer exhibits high affinity toward chloride anion and high activity owing to the close arrangement of compare to urea units compared to the *E*-isomer in several membrane transport experiments. These photomodulation systems are intriguing in developing physiological tools to study diseases related to defective transport and optopharmacological tools to stimulate neuronal activity such as halorhodopsin and rhodopsin.

3.5. Motor applications in catalysis and chemical syntheses

Enzyme catalytic reactions are well-known for their high selectivity and precision in nature. To attain this, the dynamic behavior of motors is conceivably used in catalytic reactions for better selectivity or chemical transformation. The orthogonally-responsive molecular machine as a catalyst with proper ligand arrangement anticipates the machine's future in chemical reactions. Developing a machinery-based catalyst is challenging as properly incorporating ligands with accurate dynamics must be fitted within the system, such as enzymes. The benefit of a stimuli-responsive catalyst is one that can regulate the catalytic activity as these systems offer the modulation of geometrically-distinct conformational states. Feringa's group[161] and Fletcher's group[162] separately reviewed the dynamic system's role in catalysis. Because of the extraordinary

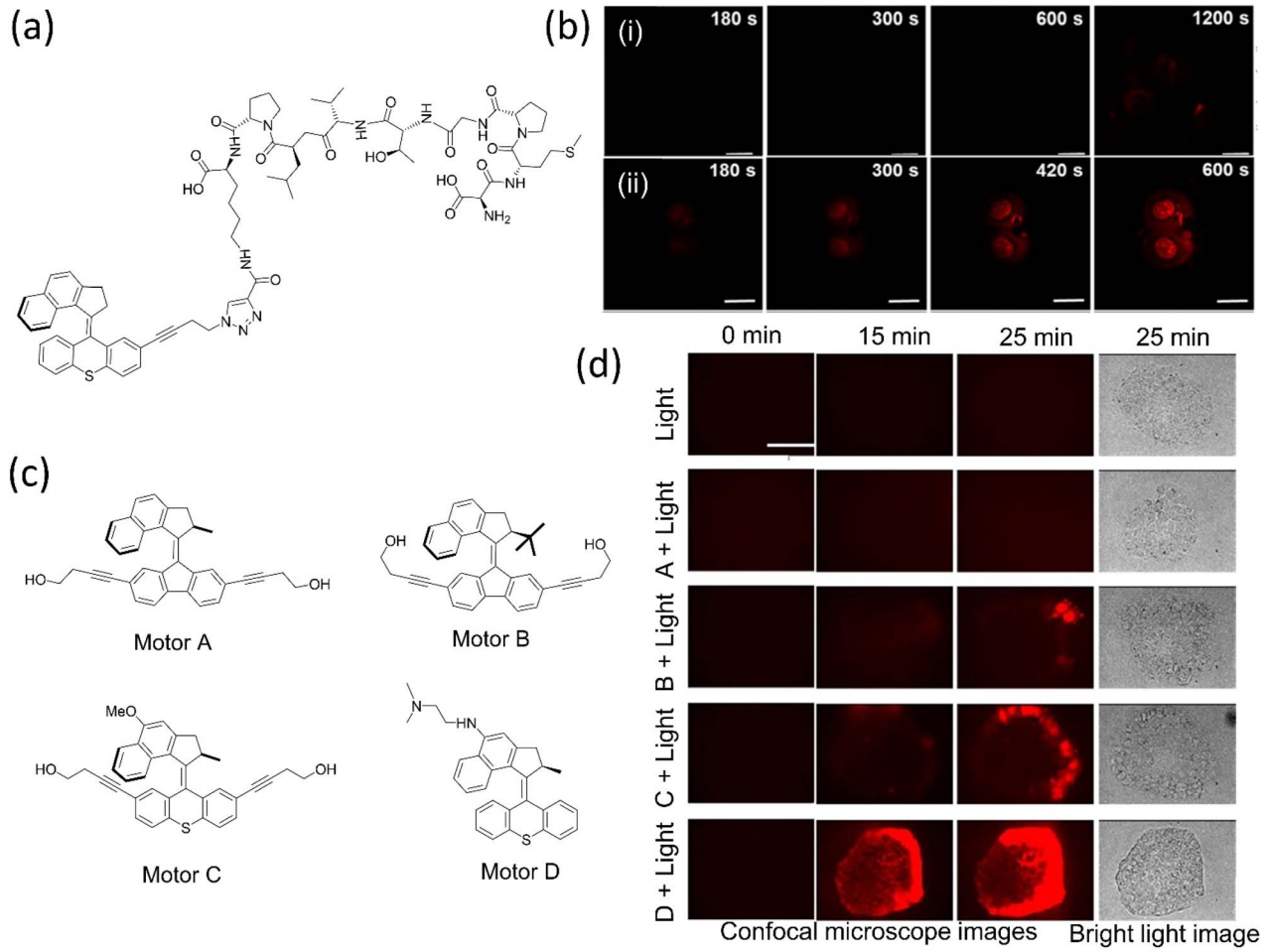

Fig. 12 (a) 2PE NIR-activated fast molecular nanomachine integrated with mono-DMPGTVLP induces cell death. (b) MCF-7–targeted nanomachine cause morphological changes and necrotic cell death on exposure to light, (i) without nanomachine, (ii) with targeted nanomachine; the scale bar in the images is 20 μm. Reproduced with permission.[153] Copyright 2019, American Chemical Society. (c) The chemical structure of visible light-activated molecular machine causes cell death through mechanical action. Among all, C and D are fast rotors. (d) Nanomechanical action of the motors on pancreatic cancer cells induces cell death. The scale bar for all the photographs is 100 μm. Reproduced with permission.[154] Copyright 2020, American Chemical Society.

advancements in this discipline over the past 20 years, very innovative designs have been created that incorporate responsive units into complex functional molecules.

Over a decade, various groups have worked on advancing motorized catalysts considering different parameters. For instance, Gilissen *et al.* developed a macrocycle system, incorporating the second-generation motor in a porphyrin system that could be used as photoswitchable catalysts exhibiting various chirality elements.[163] This motor modulates its helicity and the chiral environment, which could be used in writing binary codes 0 and 1 based on different chiralities. The inclusion of viologen guests in the motor above affected the synthesized diastereomers, which led to an acceleration of the rotational dynamics. Feringa and coworkers described the catalytic activity of the biofunctionalized first-generation motor and absolute stereoselectivity in an asymmetric conversion for the first time.[164] The stator part was tagged with thiourea, and the rotor incorporated with dimethylaminopyridine led to a bifunctional organocatalyst used in Michael additions of a 2-methoxythiophenol to 2-cyclohexene-1-one (Fig. 13a). The chirality of the motor ruled the directionality of the rotation that governed the catalytic's orientation, which determines the stereogenic center of the product. The *S*-product was obtained employing (*M*, *M*)-*Z* isomer, and the R-product with a higher yield resulted while helicity was changed from *M* to *P*. However, this catalyst shows low activity in the Henry reaction; thus, the group customized it by connecting the motor to the catalytic unit without the phenyl spacer.[165] The *Z*-isomer of the system affords the desired product with enantioselectivity up to e.e. 86 : 14. Later, to understand the role of stereoselectivity and catalyst structure, the authors developed two thiourea-functionalized catalysts for asymmetric Henry reactions (Fig. 13b).[166] The rotor tagged with an aliphatic catalytic unit showed no enantioselective control over the reaction. All the findings dictated that the catalyst structure plays a crucial role along with the rotational dynamics of the motor.

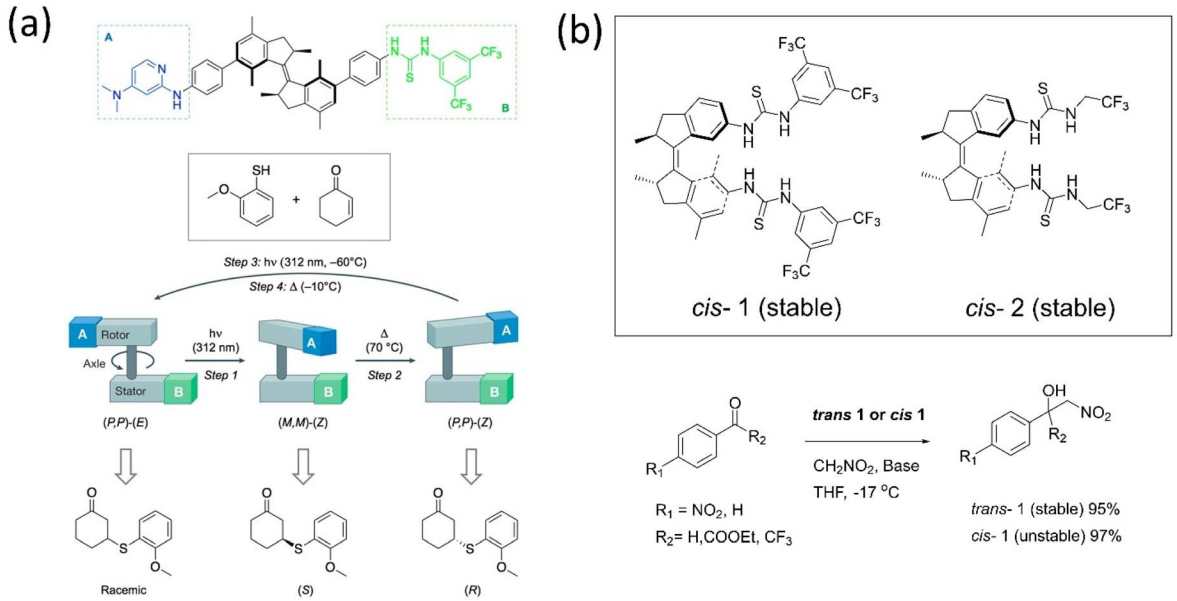

Fig. 13 (a) A bifunctional motor-based catalyst assisted the Michael addition.[164] Adapted with permission from ref. 8. Copyright 2017, Springer Nature. (b) Stable *cis* and *trans* conformer of thiourea-based catalyst. The stable and unstable catalysts 1 and 2 are employed in the Henry reaction.[166]

Transferring the specific chirality to the different elements of chirality allows the molecular motor to perform the catalytic activity.[167–170] For example, Feringa's group developed a light-driven motor-based catalyst composed of the bis(2-phenol) unit that changes its axial chirality to helical chirality (Fig. 14a).[171] The (*R*)-state of the catalyst was employed in the enantioselective addition of the diethylzinc unit into aromatic aldehyde derivatives, bringing out an enantioselective reversal product with 68%

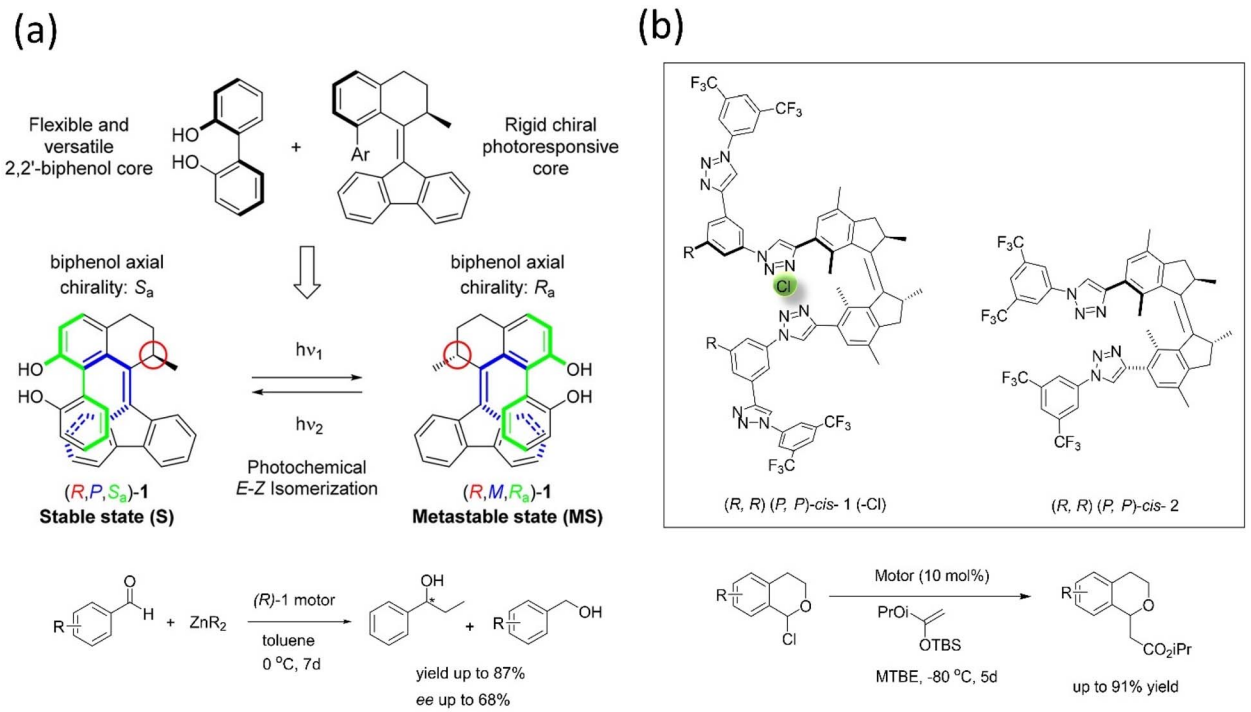

Fig. 14 (a) Dual stereo control biaryl-substituted Feringa's motor catalyst that shows an internal transfer of chirality to the coordinated metal site in an organocatalysis reaction under the light. The catalyst-mediated enantioselective addition of organozinc to aromatic aldehydes. Reproduced with permission.[171] Copyright 2018, American Chemical Society. (b) Molecular structure of the two motorized systems for stereodivergent chloride anion binding catalysis. Addition of silyl ketene acetal to 1-chloroisochroman.[172]

ee, and the yield reported was 87%. The results supported that the catalyst's chirality transfer process and allowed controlling the dynamic chirality from central to helical to axial chirality.

Dorel *et al.* reported a photoresponsive chiral catalyst based on a unidirectional molecular motor, functionalized with two oligo triazole units in each site of the system applied in anion binding.[172] These anion-binding receptor sites induce chirality in each motor's unidirectional rotation step. This motorized catalyst was employed in adding silyl ketene acetal to 1-chloroisochroman (Fig. 14b); this catalyst assists in the divergent stereoaddition of silyl ketene up to 142% Δee. The (*M*, *M*)-*cis* isomer of the catalyst produces up to 80 : 20 e.r., whereas (*P*, *P*)-*cis* state is 5 : 95 e.r. Herges and coworkers reported a novel approach to synthesizing cyclic tetravanadate *via* endogenic condensation employing an AB-based machine.[173] This system was designed by attaching two Zn-cyclene units to the AB through methylene that was bound efficiently with the reactant monovanadate, leading to the formation of the tetravanadate ring. While the system interconverts into a *cis*-isomer, it eliminates the cyclic product tetravanadate *via* hydrolysis, although it reverts to monovanadate owing to the system's stability. This example indicates that artificial molecular assemblers can change chemical synthesis paradigms such as bioproteins using the mechano-synthesis process. Based on the concept of the supramolecular process, Dube's group designed and reported a reaction of Michael addition using a hemithioindigo-based motor under visible light.[174] This motor interacted through the hydrogen bonding with the organocatalyst, namely, Schreiner's thiourea and squaramide (Fig. 15), which stopped the transformation. Still, the catalysis starts as soon as the motor adopts the *E*-conformer.

Leigh and coworkers described a motorized system capable of moving a substrate to different sites, leading to different diastereoisomer products in a chemical transformation.[175] This system comprises terminal alkene-incorporated acyl hydrazone rotor and quinoline stator bearing two prolinol silyl ethers connected by triazole linkages. The novelty of this machine is that it can stereoselectively produce one diastereomer in excess over the four products, which could not be achieved *via* the conventional method. These methods have several merits over conventional synthetic procedures, such as control over product formation. Hence, it laid the foundation for next-generation molecular machines and motors. Significant progress has been made in molecular motor-based catalysis in the last two decades, yet this field is young. The careful selection of motors with controlled dynamic motion and compatibility of the catalyst geometry are two basic parameters that offer unmatched opportunities to control a catalyst's activity and selectivity. Directing the chemical synthesis by controlling the dynamics of molecular motion will need to be explored more with structural modification, switching efficiency, and new motor design to take this sector to the next level.

3.6. Uses of molecular motors and rotors in the development of stimuli-responsive crystalline and porous materials

Porous materials provide a unique architecture for molecular motors to transform the motion at a larger scale in a solid state.

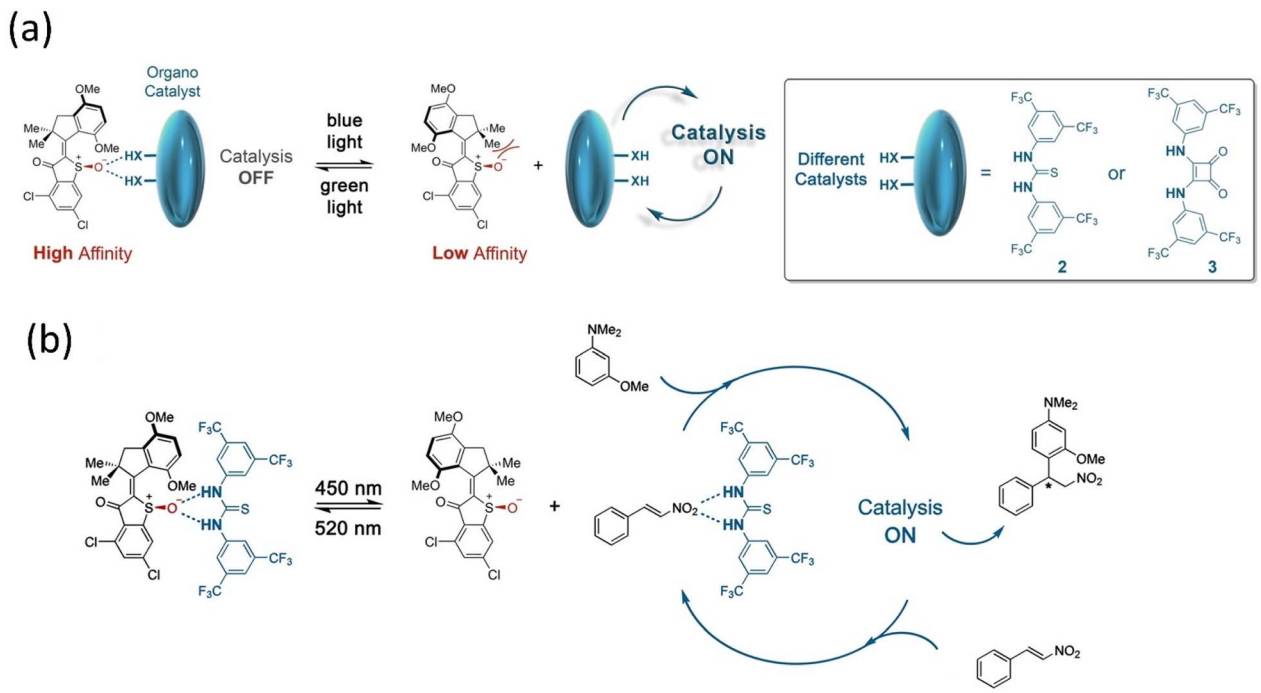

Fig. 15 (a and b) Organocatalysis of the hemithioindigo-based motor. Reproduced with permission.[174] Copyright 2020, American Chemical Society.

The incorporation of molecular rotors and motors in the solid phase is discussed briefly in Section 2.2.2. These materials offer opportunities to develop photoresponsive materials by harnessing collective motion; however, the topological change in the molecular motor may hamper the robustness of the porous materials.[176] Selectivity and separation factor might be increased by including appropriate stimuli-responsive molecules and adjusting the pore size of MOF or SURMOF (surface-mounted metal–organic framework). As a result, 3D motorized solid materials could be employed for medicine delivery, gas separation, or Li-ion battery applications. Molecular motors with ultrafast dynamics were engineered into shape-consistent, low-density porous molecular materials.[94,95,97,98] Consequently, host–guest interactions offer them to control the motor's rotational speed by interacting with diffused chemical species such as gas, liquids, or vapors.[177,178]

Perego *et al.* reported a MOF architecture integrated with two ultrafast rotors exhibiting fast mechanical motion even at 2 K temperature.[179] The two distinct rotors, bipyridine as a pillar and bicyclo[1.1.1]pentanedicarboxylate arranged in 2D layers, coordinated with the Zn-paddle wheel node, resulted in a multidynamic system. The disorder-to-order phase transitions are ascribed to the 180° flip rotation of the bipyridine (Bipy) rotor and bicyclo[1.1.1]pentanedicarboxylate (BCP) rotor that initiate multiple configurations of geared and anti-geared rotators (Fig. 16a). Notably, the low energy barrier of BCP enabled the conversation of low thermal energy into rotary motion, which could be controlled by low-pressure CO_2 gas or DMF.

Feringa, Comotti and coworkers incorporated a photoresponsive overcrowded alkene motor into porous material through the stator part to control the free volume available within the system to modulate as per conditions (Fig. 16b).[180] The system varies with inducing heat and light, leading to bulk isomerization due to the bistable rotor in the framework, which could uptake N_2 and CO_2, releasing 20% of the initial volume at a relative pressure (P/P_0) of 0.6 bar. In 2019, the group of Feringa developed a zinc pillared-paddlewheel 3D solid MOF integrating UV light-activating motors.[181] Interestingly, the unidirectional movement of the motor in the solution state is retained in the solid-state MOF as well; hence, one could expect that this system would be applicable in gas diffusion or microfluidic pumps. Different sizes of 3D metallocycles were developed by fabricating bis-pyridyl-based MPY electron-rich donor rotor with di-Pt(II) acceptors described. The metal-driven self-assembly 3D metallocycles produce a more efficient push–pull type under visible light, providing strategies for a biomimetic hierarchical system potential for generating collective motion.[182] Owing to the densely packed structure of the motor, motions are limited in the crystalline phase; however, amphidynamic crystals with molecular rotors promise solid materials that might allow conformational changes along with a change in the properties.[183] In this regard, a binuclear emissive crystalline rotor integrated with a pyrazine rotator connected to Cu or Au metal through stator NHC carbene was developed by Mingoo Jin and coworkers.[184] The length of the rotational axle connected to Au or Cu played a crucial role in controlling the rotation barrier owing to the π-accepting ability of the rotor molecule. The Cu(I) rotor complex possesses higher rotational energy and electronic delocalization than the Au (rotor), which is attributed to the higher steric interaction in the Cu(I) complex than the latter, causing a red-shifted emission in the solid state (Fig. 17). Although this system's application is not reported, these physical properties of amphidynamic crystals could be employed in pharmaceuticals, sensors, and adsorption/desorption.[185,186]

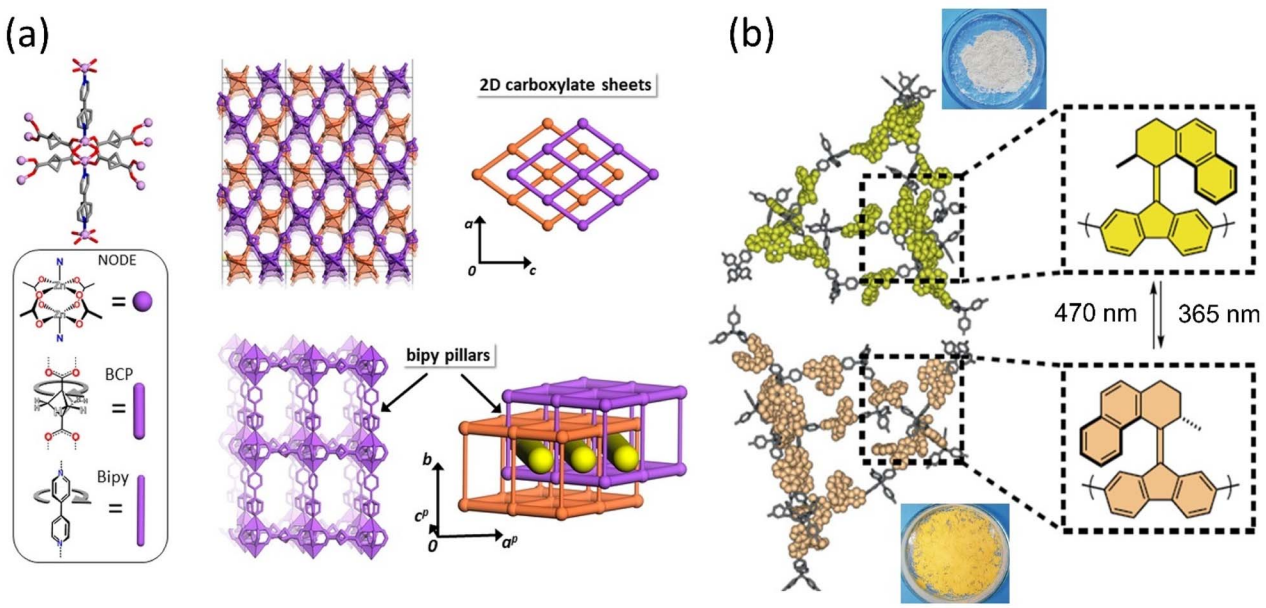

Fig. 16 (a) The component of ultrafast motorized MOF consists of Zn-paddlewheel node and molecular structures of BCP and bipy linkers and their arrangements. Reproduced with permission.[179] Copyright 2020, Springer Nature. (b) Rotary motor functionalized in MOF that changes color upon isomerization. Reproduced with permission.[180] Copyright 2020, Springer Nature.

3.7. Motor use in building stimuli-responsive soft materials and soft robotics

Through the transmission of the molecular-level nanomotion of molecular machines onto the collective motion by integrating with well-arranged networks, one could envision achieving motion such as myosin and actin filaments. Soft materials are unique functional materials that are distorted under the influence of external input and exhibit versatile features. For instance, a hydrogel could undergo shape irregularity by expansion/contraction, which is ascribed to the water releasing or retaining capacity. Stimuli-responsive and programmable shape morphing systems hold tremendous potential in biomedical, soft robotics, and biomimetic systems, thus attracting great interest. These materials are mainly functionalized with polymer, supramolecular materials, liquid crystals (LC), *etc.*, resulting in hierarchical, shape-memory, hydrogel, self-oscillating structures, and so on, especially LC-based materials and hydrogels.

Several groups successfully connected the molecular machine with supramolecular polymers and showed motion amplification at the macroscopic scale.[8,42] In 2017, a photoresponsive Feringa-created motor was incorporated into a hierarchical supramolecular assembly that shows macroscopic contractile motion.[187] An amphiphilic motor integrated with a dodecyl chain through the rotor part and stator was tagged with the carboxyl group to increase water solubility. This system undergoes a hierarchical assembly that is first assembled into the nanofiber bundle, which finally generates the long string (Fig. 18). When this string was generated under the shear flow method in an aqueous $CaCl_2$ medium, a unidirectional alignment of nanofibers and UV light exposure made the string bend toward the light. The string was able to perform a flexion angle of 90° within the 60 s in an aqueous medium with an actuation speed of $1.5 \pm 0.02°\ s^{-1}$ and with a speed of $1.8 \pm 0.07°\ s^{-1}$ in the air. The isomerization of the motor varies by local packing environment resulted in lifting a 0.4 g piece of paper on exposure to UV light. This noninvasive, light-triggered nanoscale motion is transferred to collective motion in the supramolecular assembly in water and air is envisioned to create soft robotics. Molecular motors ideally require effective chirality transfer to function from the motor part to the unit responsible for carrying out the required operation.[188] Feringa and his team provided the first example of using an overcrowded chiral alkene as the dopant by studying the transfer of photoswitchable chirality from a light-responsive molecular motor to a dynamic helical polymer to control the polymer properties. The transfer mechanism was found to be a result of the ionic interactions involving the molecular motor and helical polymers. In 2017, they reported that a dopant with photoswitchable chirality was able to bring about a preferred helicity in a poly(-phenylacetylene) polymer, which could be altered *in situ* using light stimuli.[189]

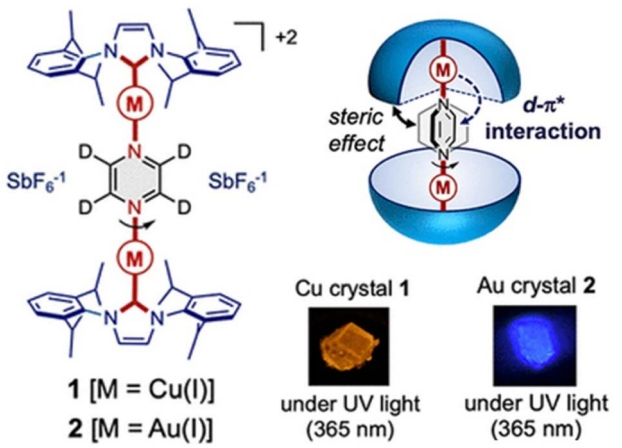

Fig. 17 Structure of the crystalline molecular rotor, the rotators are linked by metal atoms (Cu or Au). Reproduced with permission.[184] Copyright 2021, American Chemical Society.

The bottom-up approaches of integrating responsive systems with supramolecular assembly generate 3D soft matter that could amplify the molecular motion to macroscopic motion with molecular level precession. One of the approaches to achieve this is fabricating molecular rotary motors with a supramolecular assembly that combines with covalent frameworks to provide a hybrid polymer system that enables mechanical actuation at a larger scale. Giuseppone described UV-light mediated contraction of a gel framework comprising Feringa's motor.[119] These motors with a PEG chain of different molecular weights were developed, which could be used to generate eight-shaped and crosslinked gel depending upon the concentration. These systems show macroscopic work on account of the motor's rotation through the polymers' braids. However, its reversibility becomes complex as it demands massive chemical changes. In this context, the authors developed a dual light-activated system by integrating with an extra photoswitch DAE, which works overall on two different wavelengths.[120] The DAE modulator adopts a cyclic or closed form that releases the stored energy on demand. The motor stops its rotation upon irradiation with visible light. The photoswitch adopts an open form that generates free rotation around the C–C bond (Fig. 19). It releases elastic energy stored in the entangled polymer chains as kinetic energy can initiate the rotation until the system achieves thermodynamic equilibrium. The elasticity of the polymer network and osmotic pressure governed the reversible process. Taking inspiration from whirligig crafts, recently, the same group developed another system comprising a second-generation motor integrated with two polymer chains that released elastic energy from a twisted state through the reverse rotation of the strained state to a relaxed state.[190] Thus, these motorized polymeric gel systems are related to biomolecular motor-integrated muscular tissues and continuously drive away from thermodynamic equilibrium, which is more advantageous compared to molecular switch-based gel.[191]

Colin-Molina *et al.* developed a thermosalient rotor with DABCO and carbazole, showing cocrystal reversible phase transition.[192] In this system, the DABCO motif acts as a rotator, which shows fast rotation at low temperature with an activation energy of 2.6 kcal mol^{-1}. Single crystal analysis implied the phase transition process as a collective molecular displacement into macroscopic motion. The crystals were found to jump off

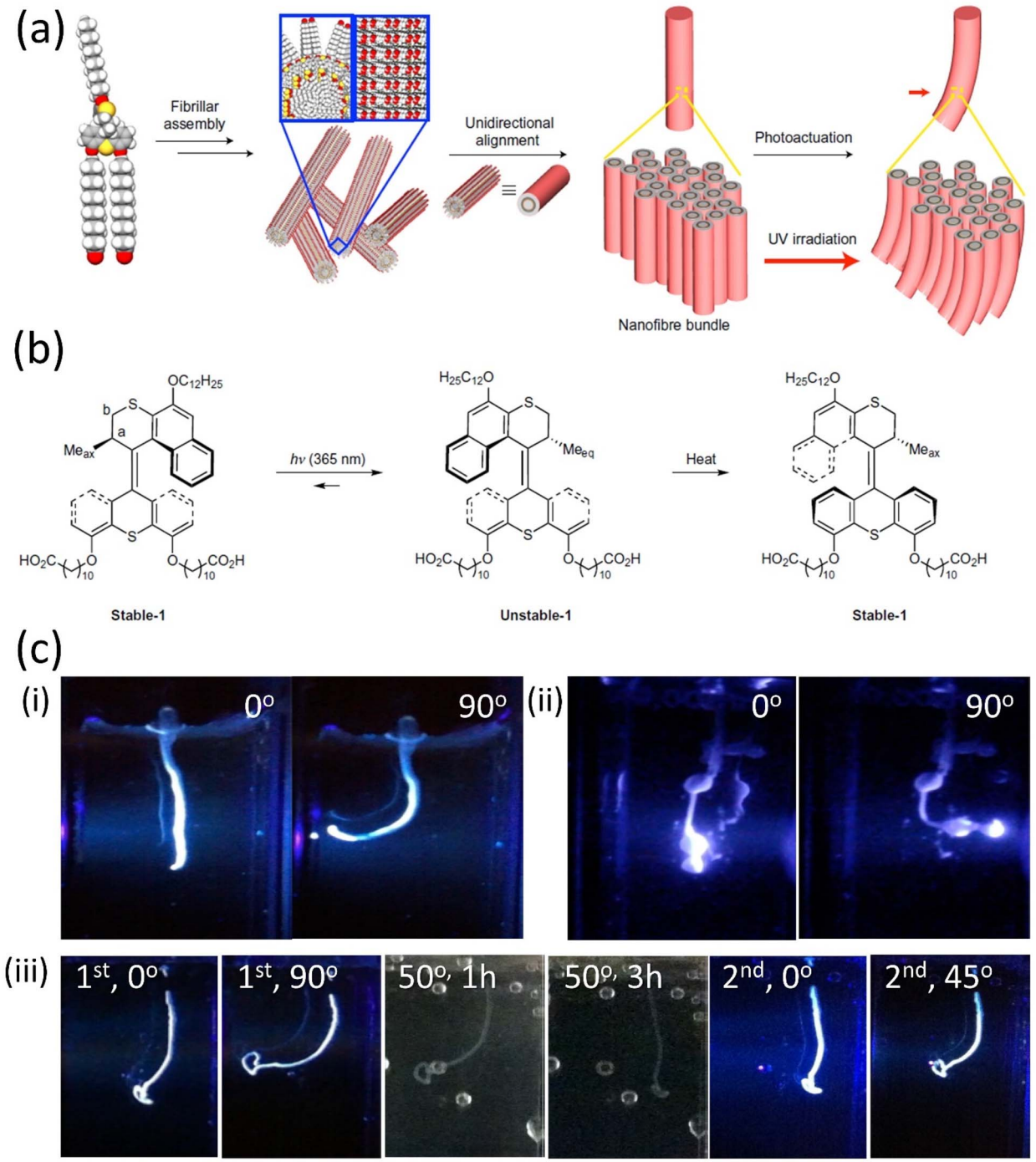

Fig. 18 (a) Graphical representation of the self-assembly of the photoresponsive molecular rotor into nanofibers, which generate a string that undergoes deformation upon exposure to UV light. (b) Photochemical and thermal helix inversion steps of the motor. Light irradiation images of different supramolecular self-assembly. (c) (i) A supramolecular string in water bends toward the direction of the UV light from 0° to 90° within 60 s; (ii) a motor string bends toward the UV light to 90° within 1 min toward the right direction; (iii) photo and thermal actuation of the motor string. The scale bars for all photographs is 0.5 cm. Reproduced with permission.[187] Copyright 2017, Springer Nature.

the surface above 316 K because of the phase transition process, resulting in changes in the rhomboid lattice of the two crystals. Thus, phase transition causes structural change, which ultimately varies the dynamics. It is the first example of a crystalline molecular machine capable of showing dynamics at the macroscopic level. Thermosensors can be constructed from such a light- and temperature-responsive material. Overall, the aforementioned working principles could be applied to create soft-phase transition materials based on rotary motors for use in molecular actuators and energy storage.[193,194]

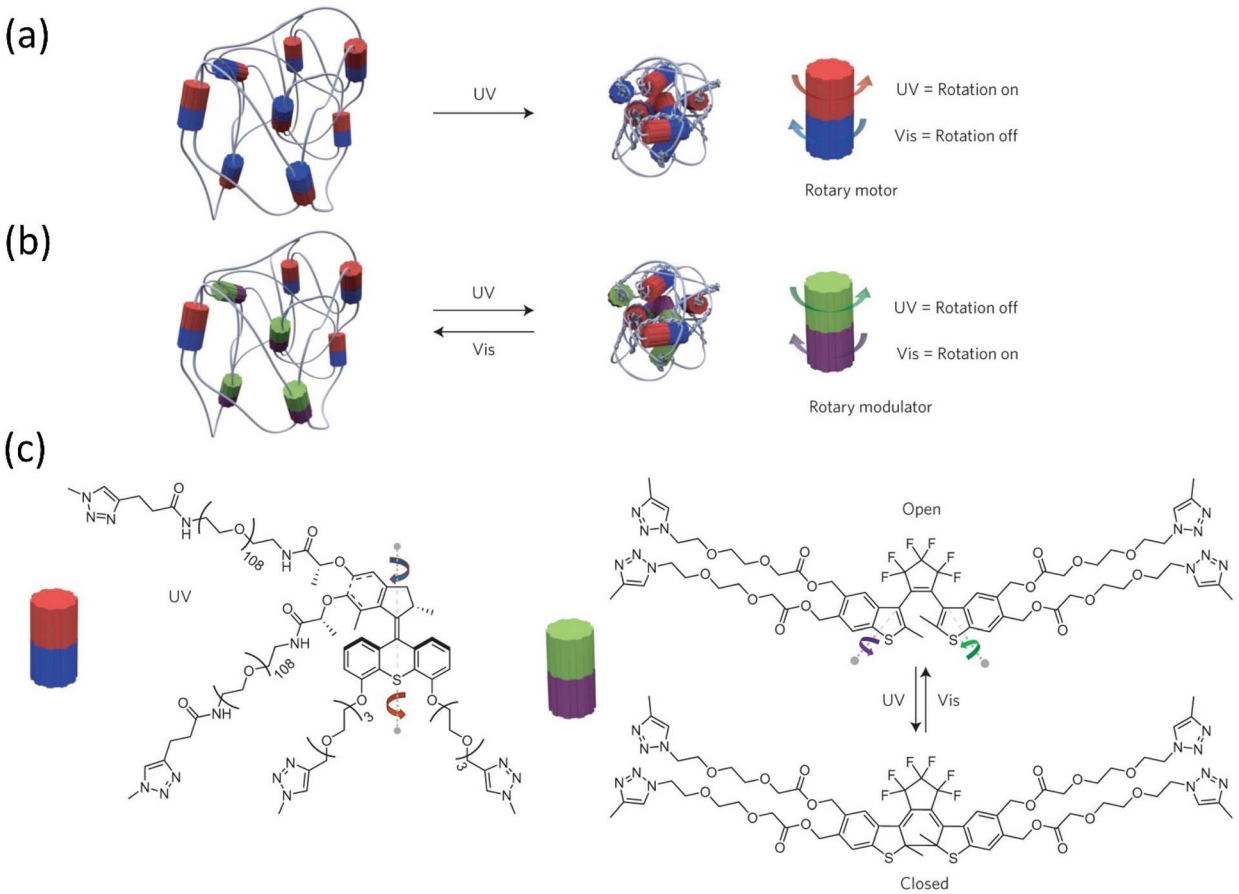

Fig. 19 Dual light control motorized modulator. Graphical representation of (a) a reticulated polymer-motor gel under UV light. (b) A polymer–motor–modulator gel. (c) Dual light control of the polymer–motor–modulator system based on enantiopure overcrowded alkenes rotor and photoswitchable dithienylethenes as the modulators. Reproduced with permission.[120] Copyright 2017, Springer Nature.

The LC materials exist between the crystalline solid-state and liquid-state, and their disordered arrangement could be aligned by applying lower energy stimuli. The long-range spatial arrangements of these thermodynamically stable LC could be achieved by interacting/combining the dynamic motion of molecular machines, which translate the nanomotion to collective motion at a certain length. It is worth mentioning that LC-based actuators can show reversible shape change in a solid state without an aqueous environment, unlike hydrogel, if they are precisely integrated with aligned molecular systems.[195] Hence, these LC-based stimuli-responsive soft materials that can magnify the external inputs into mechanical work and the future could be anticipated as an evolution of such collective motion in soft actuators, which would assist innovation in soft robotics, photonics, microfluidics, and biomedical applications.[196] For example, Katsonis and colleagues demonstrated an oscillating pattern of the motor-doped achiral LC.[197] A passive codopant was utilized to prevent the chiral-dopants' helical unwinding under light, which could produce geometrical frustration (Fig. 20a and b). When a film of the helix is enclosed between two glass slides, stimulating perpendicular orientation, this supramolecular structure was observed to impart angle-dependent propagation as the axis symmetry was disturbed. These outcomes might hold potential for developing autonomous motors that could harness light to work. Feringa's group described that a first-generation motor could transfer helices chirality into LC networks.[198] The different chiral states of the rotary motor under light can alter the geometry of the LC matrix. The system has four isomeric steps compared to the second-generation motor, which shows only two isomeric steps.[199] Thus, light can trigger the rotational steps of the motor reversibly in the macroscopic domain. The LC functionalized with a second-generation alkene motor that results in helical twisting under a single wavelength racemic motor-embedded polymeric film shows bending when induced by UV light and reverts to the initial state upon removing the source (Fig. 20c–e). Thus, a small film of the LC polymer irradiated with light results in walking or bending toward the direction of the light.

Recently, Feringa, Chen, and coworkers investigated the light-driven intricate and programmable motion of the second-generation rotary motor with an LC network.[200] The system showed fast motility and helical motion with different handedness. LC-based polymeric ribbon having four parts after UV light irradiation produced a fast wavy motion, and the motion was either against or toward the light source (Fig. 21). This actuation was due to the two different orientations of the

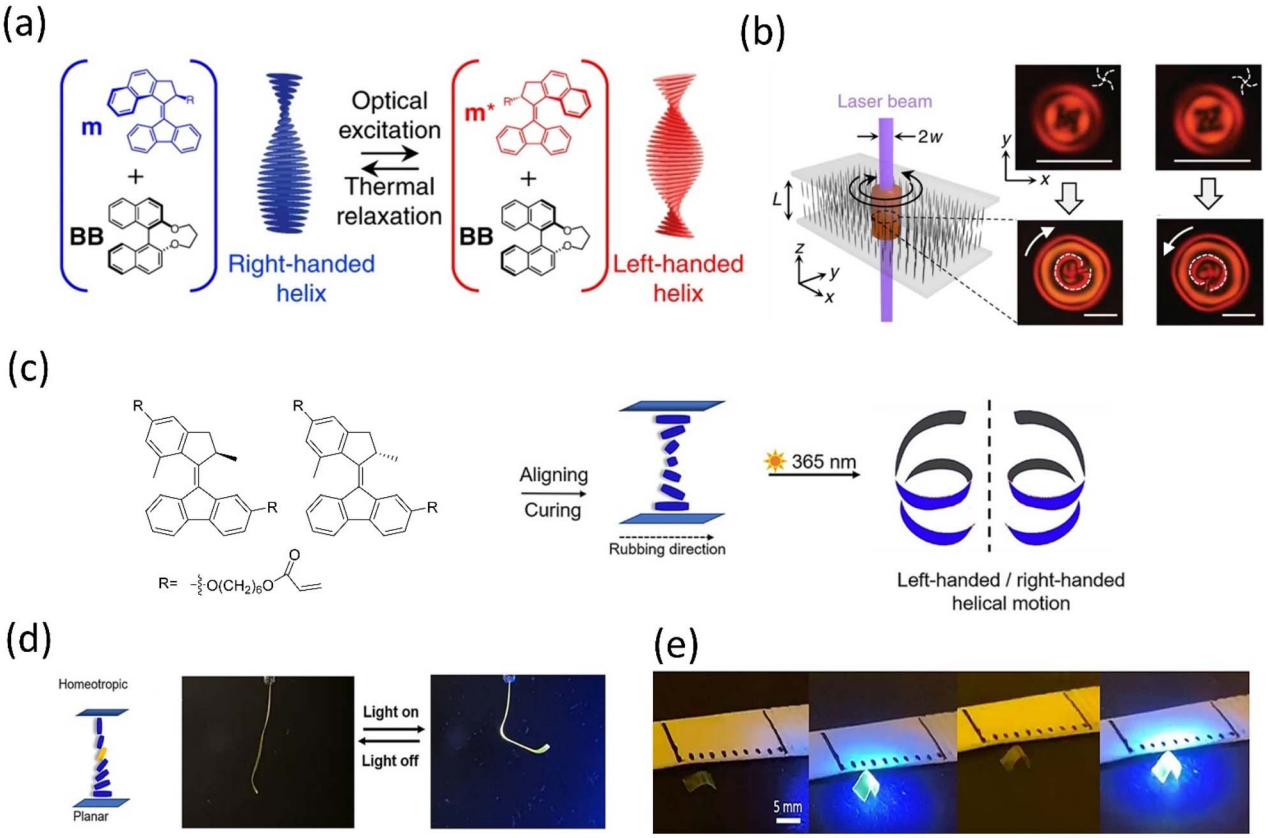

Fig. 20 (a) Molecular motor with Binol (BB) doped in LC that shows winding under light irradiation. (b) Axisymmetric chiral patterns with opposite handedness were observed by polarized optical microscopy between crossed linear polarizers. Reproduced with permission.[197] Copyright 2018, Springer Nature. (c) An enantiomerically pure molecular rotor and a mixture of these motors with LC monomer result in an indifferent helical motion. (d) Arrangement of the motor in LC monomer and its bending motion under exposure to light. (e) photoactuation of the LC ribbon on a glass surface. Reproduced with permission.[199] Copyright 2021, The Authors, published by Wiley-VCH.

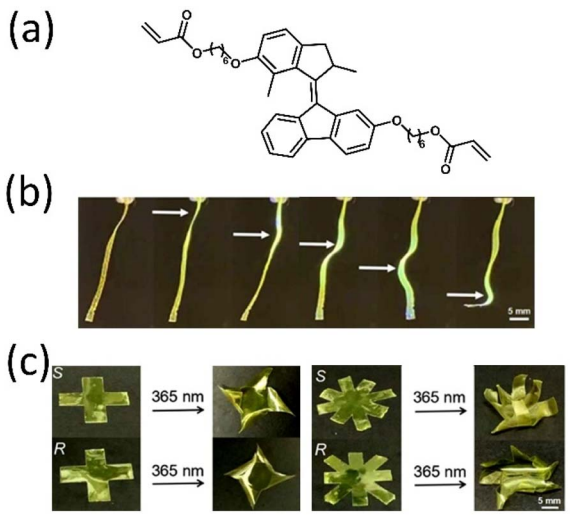

Fig. 21 (a) Molecular structure of a rotary motor. Light-powered (b) wavy motion and (c) helical motion of the motorized LC film (scale bar is 5.0 mm). Reproduced with permission.[200] Copyright 2022, The Authors, published by American Chemical Society.

racemic mixture of motors contained within the LCs network. Here, the motors play a crosslinking role in actuators; however, when enantiomerically pure motors are employed as a dopant for the LC matrix, the spiral motion was accomplished owing to the remarkable special axial chirality of the pure motor. These mentioned studies are performed employing photolithography techniques that allow the well-defined orientation of the motor and LC monomers. Hence, these studies provide the designing principles for advancing soft robotics and actuators that could generate more complex motions.

4. Some of the scope and crucial hurdles in designing artificial molecular machinery for practical use

Currently, chemists attempt to mimic autonomous natural motors to build different functional nanodevices. However, whatever molecular machines are reported to date are unlike the natural biomolecular motors and practically nonautonomous, apart from a few. One of the crucial challenges in designing the molecular machine is energy supply as the sustainable input, which operates the device, and this can be

possible be exergonic.[201] Other chemical reactions, liberating energy when cold, can be used instead. We learn from nature's creation, and our collective knowledge drives us to recreate nature's functions while maintaining thermodynamic nonequilibrium. However, at some point, if the motors fail to drive away from the thermodynamic equilibrium, we face the hurdle of bringing them back to perform their desired functions. Thus, a random synthetic approach could sometimes result in a very unrealistic outcome that often turns into failure. Therefore, the molecular modeling approach is helpful for the preliminary investigation. We can suppose that the desired dynamics in a molecular system is based on theoretical simulation data and design them accordingly. The most challenging part of developing a molecular machine is to bring a proper dynamic motion and the corresponding control on the directionality. Generally, the molecular motors follow the Brownian ratchet mechanism by exploiting random thermal motion to move; however, the motors need external input factors for their control. Therefore, a continuous power source is required for the motor to maintain operational continuity. The movement depends on the correctness of the molecular design, and the ratchet function is a critical factor for the control. Unlike macroscale machines, a molecular machine faces the interatomic forces of intramolecular attraction-repulsion within submolecular spaces. These narrow spaces consider only quantum mechanical phenomena; thus, the direct miniaturization of the classical conceptual design may not work. However, the scientist took inspiration from the natural biomachine blueprint by considering the subatomic parameters as molecular-size machines work under low Reynolds numbers and the prevailing Brownian motion conditions. Thus, one must contemplate these factors while designing the molecular machine, and the ratchet mechanism is quite helpful. Once the molecular machines' design and synthesis are over, implementation becomes vital to extract practical work from them. These systems need to be incorporated into suitable metallic or semiconducting surfaces, nanocrystals, nanoparticles, DNA scaffolds, MOFs, *etc.*, for extracting collective output to furnish the desired job.[6,8,41,202–204] The properties of molecular machines are widely exploited in the solution phase; now, the incorporation and control of their dynamics in the solid state are necessary to extract macroscopic output to develop a solid-state device. In recent times, scientists have integrated potential nanomachines on the surface materials to improve the efficiency of the collective motion of molecular machines. This was possible due to the well-defined topology of the solid materials that allow the molecule's motion to synchronize precisely. For instance, DNA scaffolds and MOFs are receiving greater attention as their free molecular spaces enable the rotary motors to rotate freely, thereby overcoming the disadvantage of the liquid crystals. The last two decades have seen a vast development in molecular machines, from surface-rolling nanocars to MOFs incorporated with molecular machines. The change in the motor's geometry could lead to a change in the geometry of the associated surface, which may benefit some systems. Nevertheless, the geometrical change in MOF due to the integrated rotor molecules might hamper the system. LC polymers are also one of the relevant surfaces for rotary motors to amplify large-amplitude rotational motion. One of the fundamental challenges in a surface grafting machine is that all the motors need to rotate freely in the desired direction without the function hindrance of adjacent molecules. In other words, there should be little or no noise; otherwise, the motor's efficiency suffers, and collective output creation fails. Further examinations of various surfaces may aid in overcoming this. The potential macroscopic applications in energy storage and release, nanorobotics, soft actuators, and the biomedical field are already visible. Although researchers have come a long way from designing a molecular machine to generating macroscopic output, several issues still need to be addressed. Properly engineering these surfaces will resolve the issues that pave the way for developing effective solutions and solid-state devices for practical applications.

5. Conclusion and perspectives

The artificial molecular machines developed in the last few decades manifest the multidisciplinary science approaches in this research field. The evolution of molecular motors has shown how these systems are introduced into materials science and chemical biology to a large extent. This review outlines different ratcheting strategies for building rotary nanomotors, their functional mechanism, and actuating properties with examples. Also, we have discussed the design of architectures that improves the performance of molecular machines at the macroscopic level to a specific scale. Moreover, we have discussed more detailed proof-of-concept to real-world implementations of diverse molecular motors, offering insights into their potential applications in various realms for future perspectives. Notably, the examples of the motors show their potential to perform or one could envision to implement in more than one application. It is captivating how far this field has come in the last two decades, from nanoscale motion to controlled cargo delivery or the movement of a droplet. The journey from the molecular level to the macroscopic scale suggests that integrating motors into different surfaces/interfaces, such as polymers, LCs, supramolecules, DNA scaffolds, and carbonaceous materials, could extract macroscopic work. Both theoretical and experimental investigations would be advantageous for designing such prototype systems.

The examples discussed here show that NIR[153] or visible light[154,174] serves as excellent stimuli. Further, the development of 2PA motors[156] or motorized nanobots[58] (*e.g.*, RF-driven) will undoubtedly be going to solve the issue related to UV-driven molecular machines. Other stimuli, such as electrical, redox, or chemical fuel, would be appropriate for the desired work. To achieve this, besides advancement in structures and architectures, a vigorous exploration of new classes of molecular motors is needed, and the library of molecular motors should increase, providing more options to engineers to develop more efficient works. In chemical synthesis, the motors may act as a robot that controls the production of different products in a programmed way.[175] Reports have been published on switching chirality; yet,

issues associated with the systems, such as the recyclability of a motor or switching activity, need to be addressed.

Thereby, many reactions will be benefited from the forthcoming rotary motor-based robotic systems. Nevertheless, manipulating other systems by molecular machines is established. This could be one of the potential areas where other classes of molecular systems should be employed to achieve nature's complexity and efficiency. A regular expression of misfolding and aggregation-prone proteins cause several diseases in human; polyglutamine expansion in different unrelated proteins are found to be responsible for many human neurodegenerative diseases. The development of dual-light active rotary motors for massive reversible elastic advantage is notable. This work may be further extrapolated to solve many such disputed biological events. For example, in prion protein disease, where protein misfolding causes severe neuro diseases, such motorized action may be helpful to repair protein misfolding, and redox-active molecular motors can inhibit the undesired polyglutamine expansion.

The development of different soft materials based on molecular motors with associated macroscopic output shows that the gap between macroscopic and molecular levels is resolving. These dynamics systems are covalently linked to the mesogen or as a chiral dopant to generate stimuli-responsive LC-based soft materials. These soft materials are quite promising as they have broad applications; yet, improvement could generate better and continuous actuation in any environment. The macroscopic actuators would be advanced by arranging hierarchical motor assemblies with supramolecular matrix using top-down and bottom-up methods such as 3D/4D printing, bundling, and layering. Flexible materials are essential for building new flexible devices; therefore, nanocage-based polymer materials having inbuilt motors may be highly futuristic to develop soft-touch materials, foldable devices, *etc.*[205] These works have perfectly shown the thoughtful design and use of molecular machine's active and passive mechanical parts. Thus, the progress accelerated toward the complexity of design to achieve more practical advantages. We have seen that silicon chip processors are expensive and high power consuming. There is great scope to design multigated rotary motors for developing high computing power processors with low energy consumption. Scientists are working on a biocomputer development where the molecular motors of biological origin are the core unit.[206] Rotary motors, if interfaced with supramolecular nanoplatform, deliver a powerful nanorobotic device that can solve very complex biocomputation and even target cancer cells with high precision, can disintegrate human Alzheimer's beta-plaque.

Another issue in the energy harvesting context is the engineering approach to device development using rotary motors to extract maximum power on a large scale. To produce maximum work, the collective output of molecular motors by cooperative nature is vital, which minimizes noise. Therefore, the assembly of molecular motors should work in unison. Thus, the different surfaces/interfaces should be put in trial and error to achieve this. To the best of our knowledge, to date, molecular rotary motors are not used in supercapacitor applications or as piezoelectricity materials. Hence, suitable functionalization with the rotary motors or exploration of rotary motors (or with different interlocked systems) in various platforms such as nanoparticles, MOFs, LCs, biomolecular scaffolds, and CQDs will undoubtedly lead to discoveries in new scientific applications.[207] The light-gated remote-functionalized photoswitching can address other motor-based photosensing devices. These remotely functionalized optical single rotary motor systems may be further extended to control multiple rotary motors with appropriate design. It is fascinating that motorized nanocars are controlled as a single molecular system and could be envisioned for high-density data processing and storage. The proper immobilization on the surface and technologies to analyze the operation of these systems at the molecular level are complex and need to be resolved. Although scientists have dominated in achieving directional motion control and converting these motions to integrated materials, many choke points to practical applications exist. The output induced by the molecular motor's collective motion would encourage scientists to construct more responsive and standalone materials. So far, several macroscopic works have been reported; the question may arise about how far this amplification of the collective motion would go by means of actuation, workload, and robustness.

Finally, as natural biomolecular motors could perform various tasks in a chaotic environment, ratcheting and engineering to develop such machines are highly desirable and challenging. One step in this direction would be the development of low-frequency active macromolecular ratchets or platforms, which can remove noises in the working frame to deliver damping-free operation. While nature has attained its complex and multifunctional machines through billions of years of evolution, forthcoming artificial molecular machinery is bright, even though its journey has not been long. Although developing a molecular motor with prototype applications is still in progress, since 1993, scientists have gradually learned to design, synthesize, and control various artificial and biomimetic molecular machines and now amplify them into collective motion. Thus, we could anticipate prominent output from molecular machinery shortly. We hope that this review will show the potential to gain knowledge and ideas to build molecular machinery (mainly rotary motors) for real-world applications.

Conflicts of interest

The authors declare there are no conflicts of interest.

Acknowledgements

The authors thank the Indian Government's DST-SERB for Grant No. ECR/2016/001534 (2017–2020). Sudeshna Kalita and Prerna Chettri are appreciative of their PhD grants from the CSIR and UGC of India. The utilities and assistance were provided by CSIR-NEIST, for which the authors are grateful. The authors appreciate the contributions of Dr Prathik Sahoo and Dr Anirban Bandyopadhyay.

Notes and references

1 M. Piccolino, *Nat. Rev.*, 2000, **1**, 149–152.
2 M. Schliwa and G. Woehlke, *Nature*, 2003, **422**, 759–765.
3 C. Mavroidis, A. Dubey and M. L. Yarmush, *Annu. Rev. Biomed. Eng.*, 2004, **6**, 363–395.
4 K. Kinosita, R. Yasuda, H. Noji, S. Ishiwata and M. Yoshida, *Cell*, 1998, **93**, 21–24.
5 R. Iino, K. Kinbara and Z. Bryant, *Chem. Rev.*, 2020, **120**, 1–4.
6 S. Erbas-Cakmak, D. A. Leigh, C. T. McTernan and A. L. Nussbaumer, *Chem. Rev.*, 2015, **115**, 10081–10206.
7 S. Corra, M. Curcio, M. Baroncini, S. Silvi and A. Credi, *Adv. Mater.*, 2020, **32**, 1906064.
8 M. Baroncini, S. Silvi and A. Credi, *Chem. Rev.*, 2020, **120**, 200–268.
9 A. W. Heard and S. M. Goldup, *ACS Cent. Sci.*, 2020, **6**, 117–128.
10 B. L. Feringa, *Angew. Chem., Int. Ed.*, 2017, **56**, 11060–11078.
11 B. L. Feringa, K. Nagatoshi, R. W. J. Zijlstra, R. A. Delden and N. Harada, *Nature*, 1999, **401**, 152.
12 M. Akter, J. J. Keya, K. Kayanoa, A. M. R. Kabir, D. Inoue, H. Hess, K. Sada, A. Kuzuya, H. Asanuma and A. Kakugo, *Sci. Robot.*, 2022, **7**, eabm0667.
13 J. J. Keya, R. Suzuki, A. M. R. Kabir, D. Inoue, H. Asanuma, K. Sada, H. Hess, A. Kuzuya and A. Kakugo, *Nat. Commun.*, 2018, **9**, 453.
14 E. Wasserman, *J. Am. Chem. Soc.*, 1960, **82**, 4433–4434.
15 C. O. Dietrich-Buchecker and J. P. Sauvage, *Tetrahedron Lett.*, 1983, **24**, 5095–5098.
16 P. L. Anelli, N. J. Spencer and J. F. Stoddart, *J. Am. Chem. Soc.*, 1991, **113**, 5131–5133.
17 R. A. Bissell, E. Cordova, A. E. Kaifer and J. F. Stoddart, *Nature*, 1994, **369**, 133–137.
18 C. P. Collier, G. Mattersteig, E. W. Wong, Y. Luo, K. Beverly, J. Sampaio, F. M. Raymo, J. F. Stoddart and J. R. Heath, *Science*, 2000, **289**, 1172–1175.
19 E. R. Kay, D. A. Leigh and F. Zerbetto, *Angew. Chem., Int. Ed.*, 2007, **46**, 72–191.
20 R. Brown, *Philos. Mag.*, 1828, **4**, 161–173.
21 R. Brown, *New Philos.*, 1828, **5**, 358–371.
22 A. Einstein, *Ann. Phys.*, 1905, **17**, 549–560.
23 J. Perrin, translated by D. L. Hammick, Constable, London, 1916.
24 D. Shi, K. Komatsu, M. Hirao, Y. Toyooka, H. Koyama, F. Tissir, A. M. Goffinet, T. Uemura and T. Fujimori, *Development*, 2014, **141**, 4558–4568.
25 S. M. King, *Dyneins: Structure, Biology and Disease*, Academic Press, 2018, pp. 162–201.
26 H. Ishikawa and W. F. Marshall, *Cold Spring Harbor Perspect. Biol.*, 2017, **1**(9), a021998.
27 I. Rayment, W. Rypniewski, K. Schmidt-Base, R. Smith, D. Tomchick, M. Benning and H. Holden, *Science*, 1993, **261**, 50.
28 N. Hirokawa, Y. Noda, Y. Tanaka and S. Niwa, *Nat. Rev. Mol. Cell Biol.*, 2009, **10**, 682.
29 S. L. Reck-Peterson, W. B. Redwine, R. D. Vale and A. P. Carter, *Nat. Rev. Mol. Cell Biol.*, 2018, **19**, 382–398.
30 H. Lodish, A. Berk, S. L. Zipursky, P. Matsudaira, D. Baltimore and J. Darnell, Photosynthetic Stages and Light-Absorbing Pigments, *Molecular Cell Biology*, W. H. Freeman, New York, 4th edn, 2000.
31 J. R. Sellers, *Biochim. Biophys. Acta, Mol. Cell Res.*, 2000, **1496**, 3–22.
32 S. Fischer, D. Horak, K. C. Holmes and J. C. Smith, *Proc. Natl. Acad. Sci. U. S. A.*, 2005, **102**, 6873–6878.
33 S. Sengupta, M. M. Spiering, K. K. Dey, W. Duan, D. Patra, P. J. Butler, R. D. Astumian, S. J. Benkovic and A. Sen, *ACS Nano*, 2014, **8**, 2410–2418.
34 A. J. Berdis, *Chem. Rev.*, 2009, **109**, 2862–2879.
35 V. Ramakrishnan, *Cell*, 2002, **108**, 557–572.
36 H. Yu, K. Jo, K. L. Kounovsky, J. J. de Pablo and D. C. Schwartz, *J. Am. Chem. Soc.*, 2009, **131**, 5722–5723.
37 C. Wang, M. P. O'Hagan, Z. Li, J. Zhang, X. Ma, H. Tian and I. Willner, *Chem. Soc. Rev.*, 2022, **51**, 720–760.
38 D. Y. Tam, X. Zhuang, S. W. Wong and P. K. Lo, *Small*, 2019, **15**, 1805481.
39 S. Mohapatra, C.-T. Lin, X. A. Feng, A. Basu and T. Ha, *Chem. Rev.*, 2019, **120**, 36–78.
40 A. Gennerich, *Nat. Nanotechnol.*, 2014, **9**, 11–12.
41 E. Moulin, L. Faour, C. C. Carmona-Vargas and N. Giuseppone, *Adv. Mater.*, 2020, **32**, 1906036.
42 A. Perrot, E. Moulin and N. Giuseppone, *Trends Chem.*, 2021, **3**, 926–942.
43 X. Yao, T. Li, J. Wang, X. Ma and H. Tian, *Adv. Opt. Mater.*, 2016, **4**, 1322–1349.
44 W. R. Bauer and W. Nadler, *J. Chem. Phys.*, 2008, **129**, 12B611.
45 R. Ait-Haddou and W. Herzog, *Cell Biochem. Biophys.*, 2003, **38**, 191–213.
46 R. D. Astumian and I. Derényi, *Biophys. J.*, 1999, **77**, 993–1002.
47 O. Kulish, A. Wright and E. Terentjev, *Sci. Rep.*, 2016, **6**, 28180.
48 R. D. Astumian, *Proc. Natl. Acad. Sci. U. S. A.*, 2007, **104**, 19715–19718.
49 F. Moss and K. Wiesenfeld, *Sci. Am.*, 1995, **273**, 66–69.
50 D. Keller and C. Bustamante, *Biophys. J.*, 2000, **78**, 541–556.
51 R. Ait-Haddou and W. Herzog, *Cell Biochem. Biophys.*, 2003, **38**, 191–213.
52 T. Strick, J.-F. Allemand, V. Croquette and D. B ensimon, *Phys. Today*, 2001, **54**, 46–51.
53 R. D. Astumian, *Nat. Commun.*, 2019, **10**, 3837.
54 H. Wang and G. Oster, *Appl. Phys. A*, 2002, **75**, 315–323.
55 W. Hwang and M. Karplus, *Proc. Natl. Acad. Sci. U. S. A.*, 2019, **116**, 19777–19785.
56 R. M. Berry, *Philos. Trans. R. Soc. London, Ser. B*, 2000, **355**, 503–509.
57 J. A. Wagoner and K. A. Dill, *J. Phys. Chem. B*, 2016, **120**, 6327–6336.
58 A. Singhania, I. Ghosh, P. Sahoo, D. Fujita, S. Ghosh and A. Bandyopadhyay, *Nano Lett.*, 2020, **20**, 6891–6898.

59 T. R. Kelly, H. De Silva and R. A. Silva, *Nature*, 1999, **401**, 150–152.
60 J. Sheng, W. Danowski, S. Crespi, A. Guinart, X. Chen, C. Stähler and B. L. Feringa, *Chem. Sci.*, 2023, **14**, 4328–4336.
61 D. Roke, S. J. Wezenberg and B. L. Feringa, Molecular rotary motors, *Proc. Natl. Acad. Sci. U. S. A.*, 2018, **115**, 9423–9431.
62 N. Koumura, R. W. J. Zijlstra, R. A. van Delden, N. Harada and B. L. Feringa, *Nature*, 1999, **401**, 152.
63 N. Koumura, E. M. Geertsema, M. B. van Gelder, A. Meetsma and B. L. Feringa, *J. Am. Chem. Soc.*, 2002, **124**, 5037.
64 J. C. Kistemaker, P. Štacko, D. Roke, A. T. Wolters, G. H. Heideman, M. C. Chang, P. Van Der Meulen, J. Visser, E. Otten and B. L. Feringa, *J. Am. Chem. Soc.*, 2017, **139**, 9650–9661.
65 T. van Leeuwen, A. S. Lubbe, P. Stacko, S. J. Wezenberg and B. L. Feringa, *Nat. Rev. Chem.*, 2017, **1**, 96.
66 D. Roke, M. Sen, W. Danowski, S. L. Wezenberg and B. L. Feringa, *J. Am. Chem. Soc.*, 2019, **141**, 7622–7627.
67 D. R. S. Pooler, R. Pierron, S. Crespi, R. Costil, L. Pfeifer, J. Leonard, M. M. Olivucci and B. L. Feringa, *Chem. Sci.*, 2021, **12**, 7486–7497.
68 G. B. Boursalian, E. R. Nijboer, R. Dorel, L. Pfeifer, O. Markovitch, A. Blokhuis and B. L. Feringa, *J. Am. Chem. Soc.*, 2020, **142**, 16868–16876.
69 A. Padwa, *Chem. Rev.*, 1977, **77**, 37–68.
70 J.-M. Lehn, *Chem. – Eur. J.*, 2006, **12**, 5910–5915.
71 L. Greb, A. Eichhöfer and J.-M. Lehn, *Angew. Chem., Int. Ed.*, 2015, **54**, 14345–14348.
72 L. Greb and J.-M. Lehn, *J. Am. Chem. Soc.*, 2014, **136**, 13114–13117.
73 M. Guentner, M. Schildhauer, S. Thumser, P. Mayer, D. Stephenson, P. J. Mayer and H. Dube, *Nat. Commun.*, 2015, **6**, 8406.
74 L. A. Huber, K. Hoffmann, S. Thumser, N. Böcher, P. Mayer and H. Dube, *Angew. Chem., Int. Ed.*, 2017, **56**, 14536–14539.
75 R. Wilcken, M. Schildhauer, F. Rott, L. A. Huber, M. Guentner, S. Thumser, K. Hoffmann, S. Oesterling, R. de Vivie-Riedle, E. Riedle and H. Dube, *J. Am. Chem. Soc.*, 2018, **140**, 5311–5318.
76 A. Gerwien, P. Mayer and H. Dube, *J. Am. Chem. Soc.*, 2018, **140**, 16442–16445.
77 S. P. Fletcher, F. Dumur, M. M. Pollard and B. L. Feringa, *Science*, 2005, **310**, 80–82.
78 B. S. Collins, J. C. Kistemaker, E. Otten and B. L. Feringa, *Nat. Chem.*, 2016, **8**, 860–866.
79 K. Mo, Y. Zhang, Z. Dong, Y. Yang, X. Ma, B. L. Feringa and D. Zhao, *Nature*, 2022, **609**, 293–298.
80 S. Borsley, E. Kreidt, D. A. Leigh and B. M. W. Roberts, *Nature*, 2022, **604**, 80–85.
81 C. García-Iriepa, M. Marazzi, F. Zapata, A. Valentini, D. Sampedro and L. M. Frutos, *J. Phys. Chem. Lett.*, 2013, **4**, 1389–1396.
82 G. Haberhauer, *Angew. Chem., Int. Ed.*, 2011, **50**, 6415–6418.
83 M. Filatov, M. Paolino, S. K. Min and C. H. Choi, *Chem. Commun.*, 2019, **55**, 5247–5250.
84 J. M. Abendroth, O. S. Bushuyev, P. S. Weiss and C. J. Barrett, *ACS Nano*, 2015, **9**, 7746–7768.
85 A. Faulkner, T. van Leeuwen, B. L. Feringa and S. J. Wezenberg, *J. Am. Chem. Soc.*, 2016, **138**, 13597–13603.
86 S. Saha, A. Ghosh, T. Paululat and M. Schmittel, *Dalton Trans.*, 2020, **49**, 8693–8700.
87 Y. Wu, G. Wang, Q. Li, J. Xiang, H. Jiang and Y. Wang, *Nat. Commun.*, 2018, **9**, 1953.
88 T. van Leeuwen, W. Danowski, S. F. Pizzolato, P. Štacko, S. J. Wezenberg and B. L. Feringa, *Chem. – Eur. J.*, 2018, **24**, 81–84.
89 A. Singhania, S. Chatterjee, S. Kalita, S. Saha, P. Chettri, F. R. Gayen, B. Saha, P. Sahoo, A. Bandyopadhyay and S. Ghosh, *ACS Appl. Mater. Interfaces*, 2023, **15**, 15595–15604.
90 D. Roke, C. Stuckhardt, W. Danowki, S. J. Wezenberg and B. L. Feringa, *Angew. Chem., Int. Ed.*, 2018, **57**, 10515.
91 L. Pfeifer, S. Crespi, P. van der Meulen, J. Kemmink, R. M. Scheek, M. F. Hilbers, W. J. Buma and B. L. Feringa, *Nat. Commun.*, 2022, **13**, 2124.
92 M. Li, S. Li, K. Zhang, X. Chi, H. Zhou, H.-B. Xu, Y. Zhang, Q. Li, D. Wang and M.-H. Zeng, *Nanoscale*, 2021, **13**, 16748–16754.
93 A. R. Hughes, N. J. Brownbill, R. C. Lalek, M. E. Briggs, A. G. Slater, A. I. Cooper and F. Blanc, *Chem.–Eur. J.*, 2017, **23**, 17217–17221.
94 G. Prando, J. Perego, M. Negroni, M. Riccò, S. Bracco, A. Comotti, P. Sozzani and P. Carretta, *Nano Lett.*, 2020, **20**(10), 7613–7618.
95 A. Comotti, S. Bracco, P. Valsesia, M. Beretta and P. Sozzani, *Angew. Chem., Int. Ed.*, 2010, **49**, 1760–1764.
96 A. Comotti, S. Bracco, T. Ben, S. Qiu and P. Sozzani, *Angew. Chem., Int. Ed.*, 2014, **53**, 1043–1047.
97 A. Comotti, S. Bracco, A. Yamamoto, M. Beretta, T. Hirukawa, N. Tohnai, M. Miyata and P. Sozzani, *J. Am. Chem. Soc.*, 2014, **136**, 618–621.
98 J. Perego, S. Bracco, M. Negroni, C. X. Bezuidenhout, G. Prando, P. Carretta, A. Comotti and P. Sozzani, *Nat. Chem.*, 2020, **12**, 845–851.
99 M. Inukai, T. Fukushima, Y. Hijikata, N. Ogiwara, S. Horike and S. Kitagawa, *J. Am. Chem. Soc.*, 2015, **137**, 12183–12186.
100 V. Balzani, A. Credi and M. Venturi, *Nano Today*, 2007, **2**, 18–25.
101 K. Ariga, *Chem. Nanomater.*, 2020, **6**, 870–880.
102 P. Ceroni, A. Credi and M. Venturi, *Chem. Soc. Rev.*, 2014, **43**, 4068–4083.
103 Here articles/newsheading related to the size of semicounductior chip: Monica Chen, Jessie Shen Hsinchu, TSMC ramping up 7 nm chip production, **https://www.digitimes.com/news/a20220323PD215.html**, June, 2018.
104 A. Gopani, *The Race to Reduce Nanometers in Chips*, **https://analyticsindiamag.com/the-race-to-reduce-nanometers-in-chips/**, January, 2022.
105 D. Burg and J. H. Ausubel, *PLoS ONE*, 2021, **16**, e0256245.
106 H. Yu, Y. Luo, K. Beverly, J. F. Stoddart, H. R. Tseng and J. R. Heath, *Angew. Chem., Int. Ed.*, 2003, **42**, 5706–5711.

107 M. M. Waldrop, *Nature*, 2016, **530**, 144.
108 N. Xin, J. Guan, C. Zhou, X. Chen, C. Gu, Y. Li, M. A. Ratner, A. Nitzan, J. F. Stoddart and X. Guo, *Nat. Rev. Phys.*, 2019, **1**, 211–230.
109 C. W. Fuller, P. S. Padayatti, H. Abderrahim, L. Adamiak, N. Alagar, N. Ananthapadmanabhan, J. Baek, S. Chinni, C. Choi, K. J. Delaney, R. Dubielzig, J. Frkanec, C. Garcia, C. Gardner, D. Gebhardt, T. Geiser, Z. Gutierrez, D. A. Hall, A. P. Hodges, G. Hou, S. Jain, T. Jones, R. Lobaton, Z. Majzik, A. Marte, P. Mohan, P. Mola II, P. Mudondo, J. Mullinix, T. Nguyen, F. Ollinger, S. Orr, Y. Ouyang, P. Pan, N. Park, D. Porras, K. Prabhu, C. Reese, T. Ruel, T. Sauerbrey, J. R. Sawyer, P. Sinha, J. Tu, A. G. Venkatesh, S. V. Kumar, L. Zheng, S. Jin, J. M. Tour, G. M. Church, P. W. Mola and B. Merriman, *Appl. Biol. Sci.*, 2022, **119**, e2112812119.
110 W. Danowski, F. Castiglioni, A. S. Sardjan, S. Krause, L. Pfeifer, D. Roke, A. Comotti, W. R. Browne and B. L. Feringa, *J. Am. Chem. Soc.*, 2020, **142**, 9048–9056.
111 A. K. Thakur, M. Majumder, S. P. Patole, K. Zaghib and M. V. Reddy, *Mater. Adv.*, 2021, **2**, 2457–2482.
112 N. I. Georgiev, N. V. Marinova and V. B. Bojinov, *J. Photochem. Photobiol., A*, 2020, **401**, 112733.
113 S. Wiedbrauk and H. Dube, *Tetrahedron Lett.*, 2015, **56**, 4266–4274.
114 M. Guentner, M. Schildhauer, S. Thumser, P. Mayer, D. Stephenson, P. J. Mayer and H. Dube, *Nat. Commun.*, 2015, **6**, 8406.
115 R. Wilcken, M. Schildhauer, F. Rott, L. A. Huber, M. Guentner, S. Thumser, K. Hoffmann, S. Oesterling, R. de Vivie-Riedle, E. Riedle and D. Henry, *J. Am. Chem. Soc.*, 2018, **140**, 5311–5318.
116 A. Gerwien, P. Mayer and H. Dube, *J. Am. Chem. Soc.*, 2018, **140**, 16442–16445.
117 Z.-Y. Zhang, Y. He, Z. Wang, J. Xu, M. Xie, P. Tao, D. Ji, K. Moth-Poulsen and T. Li, *J. Am. Chem. Soc.*, 2020, **142**, 12256.
118 L. Andreoni, M. Baroncini, J. Groppi, S. Silvi, C. Taticchi and A. Credi, *Energy Fuels*, 2021, **35**, 18900–18914.
119 Q. Li, G. Fuks, E. Moulin, M. Maaloum, M. Rawiso, I. Kulic, J. T. Foy and N. Giuseppone, *Nat. Nanotechnol.*, 2015, **10**, 161–165.
120 J. T. Foy, Q. Li, A. Goujon, J.-R. Colard-Itté, G. Fuks, E. Moulin, O. Schiffmann, D. Dattler, D. P. Funeriu and N. Giuseppone, *Nat. Nanotechnol.*, 2017, **12**, 540–545.
121 Z.-Y. Zhang, Y. He, Z. Wang, J. Xu, M. Xie, P. Tao, D. Ji, K. Moth-Poulsen and T. Li, *J. Am. Chem. Soc.*, 2020, **142**, 12256–12264.
122 G. Vives and J. M. Tour, *Acc. Chem. Res.*, 2009, **42**, 473–487.
123 J.-F. Morin, Y. Shirai and J. M. Tour, *Org. Lett.*, 2006, **8**, 1713–1716.
124 P.-T. Chiang, J. Mielke, J. Godoy, J. M. Guerrero, L. B. Alemany, C. J. Villagómez, A. Saywell, L. Grill and J. M. Tour, *ACS Nano*, 2012, **6**, 592–597.
125 A. Saywell, A. Bakker, J. Mielke, T. Kumagai, M. Wolf, V. García-López, P.-T. Chiang, J. M. Tour and L. Grill, *ACS Nano*, 2016, **10**, 10945–10952.
126 T. Jin, V. García-López, S. Kuwahara, P.-T. Chiang, J. M. Tour and G. Wang, *J. Phys. Chem. C*, 2018, **122**, 19025–19036.
127 V. García-López, P.-L. E. Chu, P.-T. Chiang, J. Sun, A. A. Martí and J. M. Tour, *Asian J. Org. Chem.*, 2015, **4**, 1308.
128 V. García-Lópeza, L. B. Alemanyad, P.-T. Chianga, J. Suna, P.-L. Chua, A. A. Martíac and J. M. Tour, *Tetrahedron*, 2017, **73**, 4864–4873.
129 T. Jin, V. García-López, P.-T. Chiang, S. Kuwahara, J. M. Tour and G. Wang, *J. Phys. Chem. C*, 2019, **123**, 3011–3018.
130 G. J. Simpson, V. García-López, A. D. Boese, J. M. Tour and L. Grill, *Nat. Commun.*, 2019, **10**, 463.
131 A. van Venrooy, V. García-López, J. T. Li, J. M. Tour and A. V. Dubrovskiy, *J. Org. Chem.*, 2020, **85**, 13644–13654.
132 G. J. Simpson, V. García-López, P. Petermeier, L. Grill and J. M. Tour, *Nat. Nanotechnol.*, 2017, **12**, 604–606.
133 P. Jacobson, D. Prezzi, D. Liu, M. Schied, J. M. Tour, S. Corni, A. Calzolari, E. Molinari and L. Grill, *J. Phys. Chem. C*, 2020, **124**, 24776–24785.
134 H. Ube, Y. Yasuda, H. Sato and M. Shionoya, *Nat. Commun.*, 2017, **8**, 14296.
135 H. Ube, R. Yamada, J. Ishida, H. Sato, M. Shiro and M. Shionoya, *J. Am. Chem. Soc.*, 2017, **139**, 16470–16473.
136 R. Asato, C. J. Martin, S. Abid, Y. Gisbert, F. Asanoma, T. Nakashima, C. Kammerer, T. Kawai and G. Rapenne, *Inorg. Chem.*, 2021, **60**, 3492–3501.
137 A. Gerwien, F. Gnannt, P. Mayer and H. Dube, *Nat. Chem.*, 2022, **14**, 670–676.
138 R. Zhao, F. Qi, Y.-L. Zhao, K. E. Hermann, R.-Q. Zhang and M. A. Van Hove, *J. Phys. Chem. Lett.*, 2018, **9**, 2611–2619.
139 R. Zhao, Y.-L. Zhao, F. Qi, K. E. Hermann, R.-Q. Zhang and M. A. Van Hove, *ACS Nano*, 2018, **12**, 3020–3029.
140 M. Baba, K. Iwamoto, R. Iino, H. Ueno, M. Hara, A. Nakanishi, J. Kishikawa, H. Noji and K. Yokoyama, *Proc. Natl. Acad. Sci. U. S. A.*, 2016, **113**, 11214.
141 Y. Zhang, J. P. Calupitan, T. Rojas, R. Tumbleson, G. Erbland, C. Kammerer, T. M. Ajayi, S. Wang, L. A. Curtiss, A. T. Ngo, S. E. Ulloa, G. Rapenne and S. W. Hla, *Nat. Commun.*, 2019, **10**, 3742.
142 J. J. Yu, Z. Q. Cao, Q. Zhang, S. Yang, D. H. Qu and H. Tian, *Chem. Commun.*, 2016, **52**, 12056–12059.
143 A. C. Coleman, J. M. Beierle, M. C. A. Stuart, B. Maciá, G. Caroli, J. T. Mika, D. J. van Dijken, J. Chen, W. R. Browne and B. L. Feringa, *Nat. Nanotechnol.*, 2011, **6**, 547–552.
144 S. Chen, F. K.-C. Leung, M. C. A. Stuart, C. Wang and B. L. Feringa, *J. Am. Chem. Soc.*, 2020, **142**, 10163–10172.
145 G. Xie, P. Li, Z. Zhao, X.-Y. Kong, Z. Zhang, K. Xiao, H. Wang, L. Wen and L. Jiang, *Angew. Chem., Int. Ed.*, 2018, **57**, 16708.
146 W. Z. Wang, L. B. Huang, S. P. Zheng, E. Moulin, O. Gavat, M. Barboiu and N. Giuseppone, *J. Am. Chem. Soc.*, 2021, **143**(38), 15653–15660.
147 J. Hou, G. Long, W. Zhao, G. Zhou, D. Liu, D. J. Broer, B. L. Feringa and J. Chen, *J. Am. Chem. Soc.*, 2022, **144**, 6851–6860.

148 A. S. Amrutha, K. R. S. Kumar, T. Kikukawa and N. Tamaoki, *ACS Nano*, 2017, **11**, 12292–12301.
149 S. Ghosh, S. Chatterjee, A. Roy, K. Ray, S. Swarnakar, D. Fujita and A. Bandyopadhyay, *Curr. Top. Med. Chem.*, 2015, **15**, 534.
150 S. Ghosh, A. Roy, A. Singhania, S. Chatterjee, S. Swarnakar, D. Fujit and A. Bandyopadhyay, *Toxicol. Rep.*, 2018, **22**, 1044–1052.
151 A. Singhania, P. Sahoo, K. Ray, A. Bandyopadhyay and S. Ghosh, *Proceedings of International Conference on Data Science and Applications*, 2020, vol. 148, p. 281.
152 V. García-López, F. Chen, L. G. Nilewski, G. Duret, A. Aliyan, A. B. Kolomeisky, J. T. Robinson, G. Wang, R. Pal and J. M. Tour, *Nature*, 2017, **548**, 567–572.
153 D. Liu, V. García-López, R. S. Gunasekera, L. G. Nilewski, L. B. Alemany, A. Aliyan, T. Jin, G. Wang, J. M. Tour and R. Pal, *ACS Nano*, 2019, **13**, 6813–6823.
154 C. A. Orozco, D. Liu, Y. Li, L. B. Alemany, R. Pal, S. Krishnan and J. M. Tour, *ACS Appl. Mater. Interfaces*, 2019, **12**, 410–417.
155 R. S. Gunasekera, T. Galbadage, C. Ayala-Orozco, D. Liu, V. García-López, B. E. Troutman, J. J. Tour, R. Pal, S. Krishnan, J. D. Cirillo and J. M. Tour, *ACS Appl. Mater. Interfaces*, 2020, **12**, 13657–13670.
156 Y. Zheng, M. K. L Han, R. Zhao, J. Blass, J. Zhang, D. W. Zhou, J.-R. Colard-Itté, D. Dattler, A. Çolak, M. Hoth, A. J. García, B. Qu, R. Bennewitz, N. Giuseppone and A. del Campo, *Nat. Commun.*, 2021, **12**, 3580.
157 L. Pfeifer, N. V. Hoang, M. Scherübl, M. S. Pshenichnikov and B. L. Feringa, *Sci. Adv.*, 2020, **6**, eabb6165.
158 S. J. Wezenberg, L.-J. Chen, J. E. Bos, B. L. Feringa, E. N. W. Howe, X. Wu, M. A. Siegler and P. A. Gale, *J. Am. Chem. Soc.*, 2022, **144**, 331–338.
159 S. J. Wezenberg and B. L Feringa, *Nat. Commun.*, 2018, **9**, 1984.
160 S. J. Wezenberg and B. L. Feringa, *Org. Lett.*, 2017, **19**, 324–327.
161 R. Dorel and B. L. Feringa, *Chem. Commun.*, 2019, **55**, 6477–6486.
162 L. van Dijk, M. J. Tilby, R. Szpera, O. A. Smith, H. A. P. Bunce and S. P. Fletcher, *Nat. Rev. Chem.*, 2018, **2**, 0117.
163 P. J. Gilissen, P. B. White, J. A. Berrocal, N. Vanthuyne, F. P. J. T. Rutjes, B. L. Feringa, J. A. A. W. Elemans and R. J. M. Nolte, *Nat. Commun.*, 2020, **11**, 5291.
164 J. Wang and B. L. Feringa, *Science*, 2011, **331**, 1429–1432.
165 M. Vlatković, L. Bernardi, E. Otten and B. L. Feringa, *Chem. Commun.*, 2014, **50**, 7773–7775.
166 M. Vlatković, J. Volarić, B. S. L. Collins, L. Bernardi and B. L. Feringa, *Org. Biomol. Chem.*, 2017, **15**, 8285–8294.
167 V. Blanco, D. A. Leigh and V. Marcos, *Chem. Soc. Rev.*, 2015, **44**, 5341–5370.
168 M. Vlatković, B. S. L. Collins and B. L. Feringa, *Chem. – Eur. J.*, 2016, **22**, 17080–17111.
169 G. Romanazzi, L. Degennaro, P. Mastrorilli and R. Luisi, *ACS Catal.*, 2017, **7**, 4100–4114.
170 D. Zhao, T. van Leeuwen, J. Cheng and B. L. Feringa, *Nat. Chem.*, 2017, **9**, 250–256.
171 S. F. Pizzolato, P. Štacko, J. C. M. Kistemaker, T. van Leeuwen, E. Otten and B. L. Feringa, *J. Am. Chem. Soc.*, 2018, **140**, 17278–17289.
172 R. Dorel and B. L. Feringa, *Angew. Chem., Int. Ed.*, 2020, **59**, 785–789.
173 H. Sell, A. Gehl, D. Plaul, F. D. Sönnichsen, C. Schütt, F. Köhler, K. Steinborn and R. Herges, *Commun. Chem.*, 2019, **2**, 62.
174 K. Grill and H. Dube, *J. Am. Chem. Soc.*, 2020, **142**, 19300–19307.
175 S. Kassem, A. T. L. Lee, D. A. Leigh, V. Marcos, L. Palmer and S. Pisano, *Nature*, 2017, **549**, 374–378.
176 T. D. Bennett, F.-X. Coudert, S. L. James and A. I. Cooper, *Nat. Mater.*, 2021, **20**, 1179–1187.
177 P. Martinez-Bulit, A. J. Stirk and S. J. Loeb, *Trends Chem.*, 2019, **1**, 588–600.
178 A. Comotti, S. Bracco and P. Sozzani, *Acc. Chem. Res.*, 2016, **49**, 1701–1710.
179 J. Perego, C. X. Bezuidenhout, S. Bracco, G. Prando, L. Marchiò, M. Negroni, P. Carretta, P. Sozzani and A. Comotti, *J. Am. Chem. Soc.*, 2021, **143**, 13082–13090.
180 F. Castiglioni, W. Danowski, J. Perego, F. K. C. Leung, P. Sozzani, S. Bracco, S. J. Wezenberg, A. Comotti and B. L. Feringa, *Nat. Chem.*, 2020, **12**, 595–602.
181 W. Danowski, T. van Leeuwen, S. Abdolahzadeh, D. Roke, W. R. Browne, S. J. Wezenberg and B. L. Feringa, *Nat. Nanotechnol.*, 2019, **14**, 488–494.
182 Z. –T. Shi, Y.-X. Hu, Z. Hu, Q. Zhang, S.-Y. Chen, M. Chen, J.-J. Yu, G.-Q. Yin, H. Sun, L. Xu, X. Li, B. L. Feringa, H.-B. Yang, H. Tian and D. -H. Qu, *J. Am. Chem. Soc.*, 2021, **143**, 442–452.
183 I. Liepuoniute, M. J. Jellen and M. A. Garcia-Garibay, *Chem. Sci.*, 2020, **11**, 12994–13007.
184 M. Jin, R. Ando, M. J Jellen, M. A. Garcia-Garibay and H. Ito, *J. Am. Chem. Soc.*, 2021, **143**, 1144–1153.
185 S. Bracco, A. Comotti and P. Sozzani, *Acc. Chem. Res.*, 2016, **49**, 1701–1710.
186 P. Naumov, D. P. Karothu, E. Ahmed, L. Catalano, P. Commins, J. M. Halabi, M. B. Al-Handawi and L. Liang, *J. Am. Chem. Soc.*, 2020, **142**, 13256–13272.
187 J. Chen, F. K.-C. Leung, M. C. A. Stuart, T. Kajitani, T. Fukushima, E. van der Giessen and B. L. Feringa, *Nat. Chem.*, 2018, **10**, 132–138.
188 J. Chen, S. J. Wezenberg and B. L. Feringa, *Chem. Commun.*, 2016, **52**, 6765–6768.
189 T. van Leeuwen, G. H. Heideman, D. Zhao, S. J. Wezenberg and B. L. Feringa, *Chem. Commun.*, 2017, **53**, 6393–6396.
190 C. Gao, A. V. Jentzsch, E. Moulin and N. Giuseppone, *J. Am. Chem. Soc.*, 2022, **144**, 9845–9852.
191 J.-R. Colard-Itté, Q. Li, D. Collin, G. Mariani, G. Fuks, E. Moulin, E. Buhler and N. Giuseppone, *Nanoscale*, 2019, **11**, 5197–5202.
192 A. Colin-Molina, D. P. Karothu, M. J. Jellen, R. A. Toscano, M. A. Garcia-Garibay, P. Naumov and B. Rodríguez-Molina, *Matter*, 2019, **1**, 1033–1046.

193 F. Long, Y. Cheng, Y. Ren, J. Wang, Z. Li, A. Sun and G. Xu, *Adv. Eng. Mater.*, 2022, **24**, 2100863.
194 Y. Zheng, X. Jia, K. Li, J. Xu and X. H. Bu, *Adv. Energy Mater.*, 2022, **12**, 2100324.
195 W. Feng, D. Liu and D. J. Broer, *Small Struct.*, 2021, **2**, 2000107.
196 D. Martella, P. Paoli, J. M. Pioner, L. Sacconi, R. Coppini, L. Santini, M. Lulli, E. Cerbai, D. S. Wiersma, C. Poggesi, C. Ferrantini and C. Parmeggiani, *Small*, 2017, **13**, 1702677.
197 T. Orlova, F. Lancia, C. Loussert, S. Iamsaard, N. Katsonis and E. Brasselet, *Nat. Nanotechnol.*, 2018, **13**, 304–308.
198 A. Ryabchun, F. Lancia, J. Chen, D. Morozov, B. L. Feringa and N. Katsonis, *Adv. Mater.*, 2020, **32**, 2004420.
199 J. Hou, A. Mondal, G. Long, L. de Haan, W. Zhao, G. Zhou, D. Liu, D. J. Broer, J. Chen and B. L. Feringa, *Angew. Chem., Int. Ed.*, 2021, **60**, 8251–8257.
200 J. Hou, G. Long, W. Zhao, G. Zhou, D. Liu, D. J. Broer, B. L. Feringa and J. Chen, *J. Am. Chem. Soc.*, 2022, **144**, 6851–6860.
201 A. Credi, *J. Phys.: Condens. Matter*, 2006, **18**, S1779.
202 C. Wang, M. P. O' Hagan, Z. Li, J. Zhang, X. Ma, H. Tian and I. Willner, *Chem. Soc. Rev.*, 2022, **51**, 720–760.
203 A. S. Lubbe, Q. Liu, S. J. Smith, J. Willem de Vries, J. C. M. Kistemaker, A. H. de Vries, I. Faustino, Z. Meng, W. Szymanski, A. Herrmann and B. L. Feringa, *J. Am. Chem. Soc.*, 2018, **140**, 5069–5076.
204 E. Kolodzeiski and S. Amirjalayer, *Phys. Chem. Chem. Phys.*, 2021, **23**, 4728–4735.
205 A. Dhamija, C. K. Das, Y. H. Ko, Y. Kim, R. D. Mukhopadhyay, A. Gunnam, X. Yu, I. C. Hwang, L. V. Schäfer and K. Kim, *Chem*, 2022, **8**, 543–556.
206 D. V. Nicolau Jr, M. Lard, T. Korten, F. C. Van Delft, M. Persson, E. Bengtsson, A. Månsson, S. Diez, H. Linke and D. V. Nicolau, *Proc. Natl. Acad. Sci. U. S. A.*, 2016, **113**, 2591–2596.
207 Z. Liu, H. I. Wang, A. Narita, Q. Chen, Z. Mics, D. Turchinovich, M. Kläui, M. Bonn and K. Müllen, *J. Am. Chem. Soc.*, 2017, **139**, 9443–9446.